

FERMILAB-Proposal-0595

CALT Proposal 68-638

Caltech/Rochester/Stanford Proposal

A STUDY OF CHARM AND OTHER NEW FLAVORS PRODUCED  
IN PION-NUCLEON COLLISIONS

B. C. Barish, J. F. Bartlett, K. W. Brown, R. L. Messner,

M. H. Shaevitz, E. J. Siskind

California Institute of Technology, Pasadena, California 91125

A. Bodek, W. Marsh, J. Ritchie, S. Olsen

University of Rochester, Rochester, New York 14627

and

G. Donaldson, F. S. Merritt, S. Wojcicki

Stanford University, Stanford, California 94305

January 1978

Scientific Spokesperson:

A. Bodek  
University of Rochester  
716/275-3929

15 pages

Table of Contents

	<u>Page</u>
Summary	4
Introduction	6
Part I. Low Intensity Running (Investigation of the Low $P_t$ Region)	
1. Theory (charm)	9
2. Sensitivity and Comparison with Models	13
3. Physics Goals, low intensity running.	16
4. Apparatus	17
5. Event Rates	29
6. Backgrounds and Analysis - low $P_t$ running.	30
Part II. High Intensity Running (High $P_t$ Region and Multimuons)	
1. Introduction - Heavy Flavor Production	34
2. Theory (bottom states)	35
3. Physics Goals, high intensity running.	42
4. Event Topologies and Rates, high $P_t$ running.	43
5. Triggers Background and Analysis, high intensity running.	44
6. Acceptance and Efficiencies.	49
7. Summary: high intensity running.	51
References (Parts I and II)	52
Appendix A: Decay Modes of Bottom Particles.	58
Appendix B: Acceptance Calculations - high $P_t$ running.	60

Figures

		<u>Page</u>
Part I.	1. The present state of experiments hunting for bare bottom states.	8
	2. Cross Sections for $K \bar{K}$ and $\phi$ Production versus Energy.	10
	3. Theoretical Charm Production Cross Sections for PP.	14
	4. Theoretical Charm Production Cross Sections for $\pi P$ .	15
	5. Calorimeter Resolution at 400 GeV.	19
	6. Calorimeter Resolution at 400 GeV (semilog plot).	20
	7a. Calorimeter Resolution versus Energy.	21
	7b. Calorimeter Calibration versus Energy.	22
	8. Old E-379 Setup.	24
	9. New Experimental Setup.	25
	10. Observed $\psi$ Peak in E-379.	27
	11. $P_t$ Distributions for Muons from Charm Decays.	32
Part II.	1. Pion Upsilon Production Cross Sections versus Energy.	39
	2. X Distributions in Low Energy $\psi$ Production by Pions.	40
	3. X Distributions for Upsilon Production by Pions.	41
	4. $P_t$ Distributions for Muons from Charm and Bottom Particle Decays.	46
	5. $P_t$ versus $P_{  }$ Acceptance Plot in the Lab Frame (focussing muons).	63
	6. $P_t$ versus $P_{  }$ Acceptance Plot in the Lab Frame (defocussing muons).	64
	7. $P_t$ versus $P_{  }$ Acceptance Plot in the Center of Mass (250 GeV pions) for focussing muons.	65

Summary

We propose to perform an investigation of charm production in pion nucleon collisions. The experiment is a continuation of Experiment E-379 which performed a similar investigation of new states produced in proton-nucleon collisions. The experiment investigates short lived states decaying weakly via leptonic (or semi-leptonic) modes. In addition, the second part of the experiment will have a first look at the high  $P_t$  region where heavy state (i.e. bottom) production is expected to show up. Our preliminary study indicates that such a search in the E-379 detector looks promising. However, to reach the desired sensitivity would require a very long run. It is, therefore, our intention to have a preliminary look at that region before proposing to undertake a detailed search.

The experiment will use the existing E-379 calorimeter placed upstream of the 12' muon spectrometer. The calorimeter will act simultaneously as a target and will give an accurate energy measurement ( $\Delta E/E$  was measured to be 3.5% at 400 GeV). The unique features of the experiment are the detection of missing energy (presumably carried off by neutrinos) and a wide solid angle acceptance for muons. The modifications of the old E-379 setup will make use of a part of the recently constructed E-356 neutrino target to extend the muon identification to virtually the complete  $4\pi$  solid angle in the center of mass. We propose the running be scheduled during horn cycles when the neutrino experiment in Lab-E is normally off.

We are requesting approval for the use of the N5 beam line for a period of one horn cycle (10 weeks). The time will be divided between a low  $P_t$  (charm) period and a high  $P_t$  (heavy flavors) period as follows:

2 weeks	checkout
4 weeks (400 hours)	Low $P_t$ running
	$10^5 \pi^-$ /pulse at 300 GeV

1 week	change to a high $P_t$ configuration
3 weeks (300 hours)	High $P_t$ running
	$10^6 \pi^-$ /pulse at 250 to 300 GeV.

The first 400 of data will be used to investigate the low  $P_t$  region. A relatively low intensity negative pion beam ( $\approx 10^5$ /pulse) at the highest beam energy ( $\approx 300$  GeV) will be used. The total cross section for charm production will be measured as well as the X dependence of the production. Also, some information on the production  $P_t$  characteristics may also be obtained.

The other 300 hours of data will be taken at  $10^6$  pions/pulse and will be used to obtain a first look at the possible production of new heavy flavors in pion nucleon collisions. A preliminary survey in this unexplored region will search for new phenomena, and according to some theoretical models, may have the sensitivity to detect bottom states. Our own calculations indicate that a run of about 1600 hours at  $10^6$  pions/pulse is needed to measure the anticipated cross section for the production of bottom states. Uncertainties in the backgrounds production cross sections, etc., preclude a definite commitment to such a long run until results of the survey run are available.

## INTRODUCTION

The existence of charmed particles is firmly established at this time, mainly through the observation of bare charm in  $e^+e^-$  machines<sup>1</sup>, as well as signatures in real and virtual photon<sup>2</sup>, and neutrino reactions.<sup>3</sup> The measurement of charm production cross section with hadron beams has proven to be difficult and no successful experiments have been reported. Similarly, although the newly discovered<sup>4</sup> T is expected to be a signature of a hidden new flavor (e.g. bottom) no observation has been reported of bare bottom states. The apparatus of Fermilab Experiment E-379 has the sensitivity to measure the expected charm production cross sections and may go as far as to be able to measure the X-distribution of the produced states and may yield some information on the production  $P_t$  characteristics. The feasibility for detection of bare bottom states looks promising. At present, among other proposed experiments, only the future  $e^+e^-$  machines may detect bare bottom states. Presently no proposals have been made to measure the production of such states with hadron beams. A summary of the present state of experiments to look for bare bottom states, which has been recently presented in the December 1977 issue of the CERN Courier, is shown in Figure 1.

Experiment<sup>5</sup> E-379 had a first run with 400 GeV protons. Preliminary results of that run will be presented elsewhere.

We propose a second run with incident pions, using the E-379 apparatus (with small modifications for improved sensitivity) to determine the total cross sections and production characteristics of charmed particles produced in pion-nucleon collisions. A first survey of the heavy state region (e.g. bottom) will be performed to determine the experimental backgrounds in that region and place limits on the production cross sections of such states. The results of that survey will be used to determine whether a longer run to determine the production cross sections of such states should be undertaken.

The experiment is expected to yield results shortly after running because all the software programs have been developed for the proton run.

We utilize two signatures for detecting weak decays. One is a single muon signal (with no other visible muon) which is determined to be direct (via a density comparison) and associated with missing energy. The other is a two muon signal which is associated with missing energy. The latter results from the weak decays of two particles. In addition, multimMuon states with and without missing energy will be studied.

Our approach for the detection of hadronic produced states which decay weakly differs substantially from the approaches taken by other experiments. We are also sensitive to other processes which may yield muons and neutrinos in the final states and thus complement the approaches of other investigations. These latter approaches include hunting for mass bumps such as  $k\pi$  resonances, detecting  $\mu e$  events and searching for short tracks in emulsion or streamer chamber experiments. Unfortunately, none has yielded positive results as of the present time.

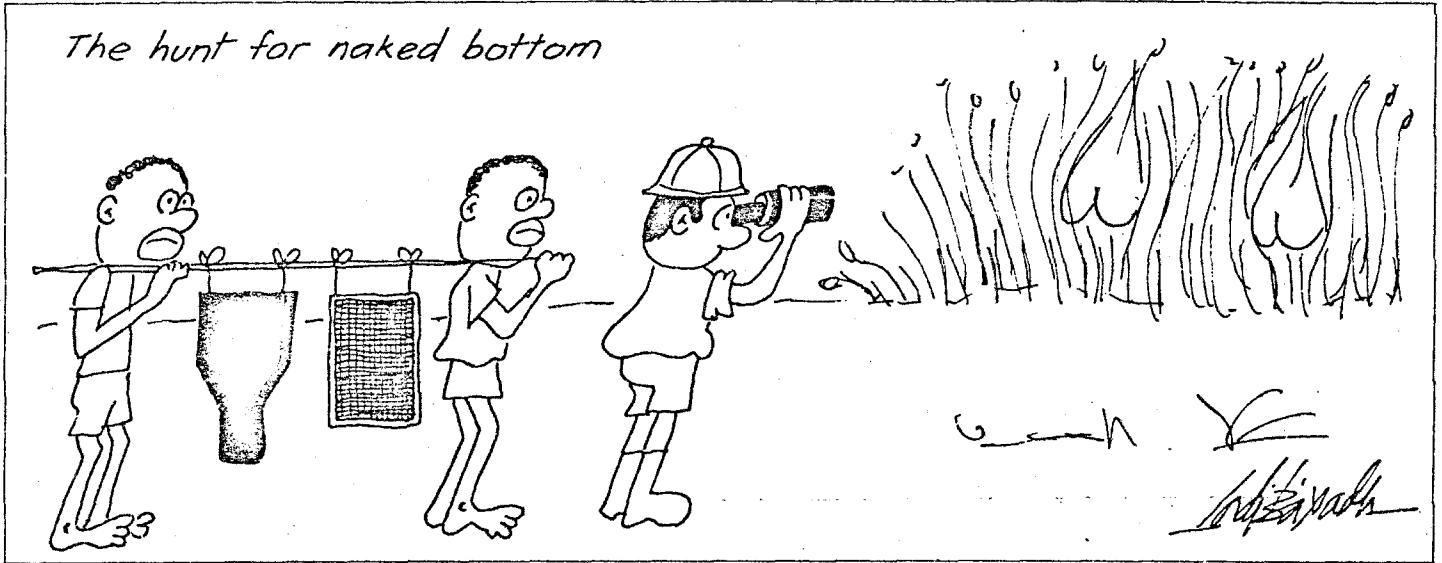


FIG. 1

The present state of experiments - hunting for bare bottom states (from the December 1977 issue of the CERN Courier).

Part I: Low Intensity Run (investigation of the low  $P_t$  region)

Theory (Charm)

The measurement of charm and other heavy particle production cross sections with pion and proton beams provides valuable information for understanding the general process of hadronic interactions and the processes of particle production in particular. Such data, for example, are particularly useful in testing the framework of the quark-gluon color gauge field theory<sup>6</sup> (QCD). This is because heavy particle production is much less sensitive to the lower mass divergences and, therefore, can be calculated using the same techniques as the lepton production calculations as well as the calculation of  $e^+e^-$  cross sections.

The heavy particle production processes complement our knowledge of the structure of hadrons because both gluon-gluon and quark-antiquark processes contribute. Other process such as  $e^+e^-$  annihilation, electron, muon, and neutrino interactions and lepton pair production in hadron collisions provide detailed information on quark and antiquark distributions but only qualitative results on gluon contributions. The latter, for example, are that gluon carry roughly 50% of the nucleon's momentum and that gluons participate in "radiative type" corrections that lead to such things as scaling violations.

On the other hand, heavy particle production yields information both on quark and gluon contributions, and the separate contributions may be studied by measurements of heavy particle production cross sections as a function of energy and particle type as well as measurements of the production  $X_F$  distributions. In particular, since incident pions have a larger antiquark content than protons, pions are expected to have a larger charm production cross section and also exhibit a flatter  $X_F$  distribution.

Setting specific models aside, we obtain an estimate of charm production cross section using the following relation<sup>7</sup>

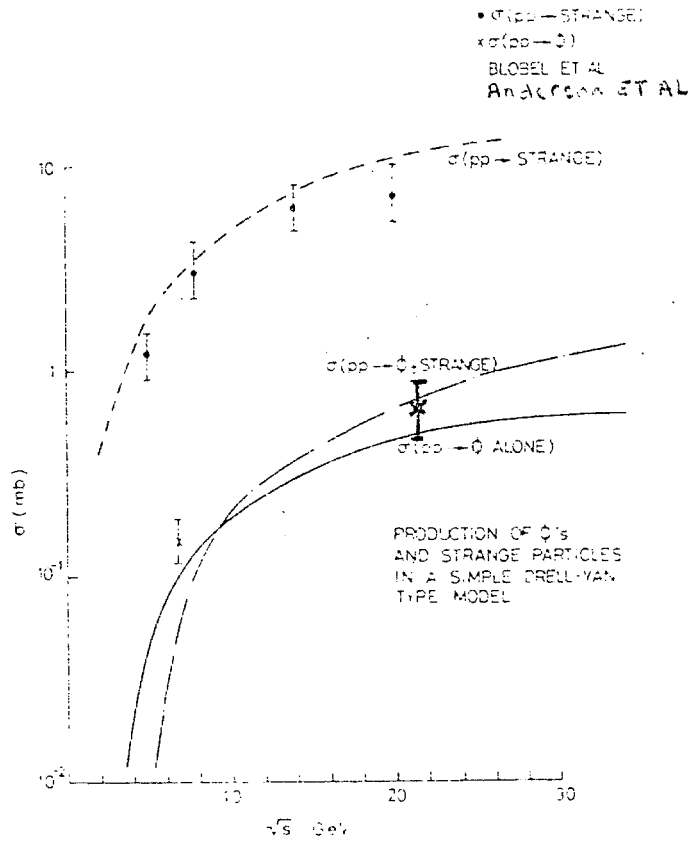


FIG. 2

Calculated  $\sigma(pp \rightarrow \text{strange})$  and  $\sigma(pp \rightarrow \phi)$  cross sections from D. Sivers, Nucl. Phys. B106, 95 (1976). Data points are from V. Blobel et al. Phys. Lett. 59B, 88 (1975) and K. J. Anderson et al., Phys. Rev. Lett. 37, 799 (1976).

$$\frac{\sigma_{\text{bottom}}}{\sigma_{\text{T}}} \approx \frac{\sigma_{\text{charm}}}{\sigma_{\psi}} \approx \frac{\sigma_{\text{KK}^-}}{\sigma_{\phi}} \approx 10$$

where the ratio  $\sigma_{\text{KK}^-}/\sigma_{\phi} = 10$  for protons obtained from the available data shown in Figure 2.

Using the branching ratio<sup>8</sup>  $\psi \rightarrow \mu^+ \mu^-$  of  $(7.5 \pm 0.5)\%$  and the measured<sup>9,10</sup> J/ $\psi$  cross sections  $B \cdot \sigma_{\text{T}}(\psi)$  [taking  $\sigma_{\text{T}} = 2\sigma$  ( $x > 0$ ) and an  $A^{1.0}$  dependence] of  $13 \times 10^{-33} \text{ cm}^2/\text{nucleon}$  for 150 GeV  $\pi^+ \text{N}$  and  $20 \times 10^{-33} \text{ cm}^2/\text{nucleon}$  and  $24 \times 10^{-33} \text{ cm}^2/\text{nucleon}$  for 225 GeV  $\pi^+ \text{N}$  and  $\pi^- \text{N}$  respectively we obtain the following charm production cross sections.

Particle	Energy	$\sqrt{s}$	Expected Charm Cross Section/Nucleon
			Isoscalar Target
$\pi^+$	150 GeV	16.8	$1.7 \times 10^{-30} \text{ cm}^2$
$\pi^+$	225 GeV	20.6	$2.7 \times 10^{-30} \text{ cm}^2$
$\pi^-$	225 GeV	20.6	$3.2 \times 10^{-30} \text{ cm}^2$

Similarly, using the measured<sup>9,10</sup> cross sections  $B \cdot \sigma_{\psi}$  of  $6.6 \times 10^{-33} \text{ cm}^2/\text{nucleon}$  and  $14 \times 10^{-33} \text{ cm}^2/\text{nucleon}$  for 150 GeV and 225 GeV protons respectively, we obtain charm production cross sections of  $0.9 \times 10^{-30} \text{ cm}^2/\text{nucleon}$  and  $1.9 \times 10^{-30} \text{ cm}^2/\text{nucleon}$  for 150 GeV and 225 GeV protons respectively. Using the energy dependence<sup>10</sup> of the cross sections  $(\frac{d\sigma}{dy})(y=0)$  for  $\psi$  production we also obtain charm cross sections of  $(2.9 \text{ to } 3.8) \times 10^{-30} \text{ cm}^2/\text{nucleon}$  for charm production in 400 GeV proton-nucleon collisions.

The fact that the  $\psi$  production cross section for pions are about twice the proton cross sections as well as the observed flatter X dependence<sup>9,10</sup> for pion  $\psi$  production [  $(1-X)^{1.3}$  for pions versus  $(1-X)^{3.4}$  for protons] may indicate that the quark-antiquark process may contribute a larger fraction to both the  $\psi$  and charm production cross sections.

The above charm cross sections are still well below recently reported limits for  $D\bar{D}$  production cross sections. There are  $\sigma_{D\bar{D}} < 2.8 \times 10^{-29} \text{ cm}^2/\text{nucleon}$  for 250 GeV neutrons<sup>11</sup>,  $\sigma_{D\bar{D}} < 2.6 \times 10^{-29} \text{ cm}^2/\text{nucleon}$  for 400 GeV protons<sup>12</sup>, and  $\sigma_{\text{charm}} < 1.5 \times 10^{-29} \text{ cm}^2/\text{nucleon}$  for 300 GeV neutrons<sup>13</sup>. The cross sections are of the same order of a recent emulsion experiment limit<sup>15</sup> of  $\sigma_{\text{charm}} < 1.5 \times 10^{-30} \text{ cm}^2$  for 300 GeV protons. In that experiment, however, the results are sensitive to assumptions about the charm states lifetimes.

Another limit can be obtained from data<sup>16</sup> of the Chicago-Princeton group which finds that for 200 GeV protons  $0.7 \pm 0.2$  of all prompt muons are produced in pairs for  $X > 0.1$  and  $P_t < 1 \text{ GeV}$ . Assuming that this ratio is the same near  $X \approx 0$  we get that  $\leq 0.3 \pm 0.2$  of all prompt muons may come from other sources (e.g. charm). Using  $\sigma_{2\mu} \simeq 5 \times 10^{-30} \text{ cm}^2/\text{nucleon}$  and a branching ratio of 0.15 for the charm decay we obtain  $\sigma_{\text{charm}} \leq 1.0 \times 10^{-29} \text{ cm}^2/\text{nucleon}$ .

Sensitivity and Comparison with Models

If our estimate of the charm production cross section of  $4 \times 10^{-30}$  is correct, then information on the X and  $P_t$  production distributions can be extracted from the data. If the cross sections are a factor of 10 lower, than probably only total cross sections can be determined. The sensitivity of the experiment is limited by how well the pion and kaon decay backgrounds are determined (in the case of the single muon signature). Cuts on  $P_t$  and  $E_\mu$  as well as missing energy cuts can be used to reduce the level of this background and the density comparison data to determine the remaining background after the cuts. We estimate that this background will limit our ability to measure charm cross sections (assuming BR of  $D \rightarrow \mu\nu$  of 12%)<sup>38</sup> to  $\sigma_{total}^{charm} \geq 3 \times 10^{-31} \text{ cm}^2$ <sup>41</sup> (the background from misidentified  $2\mu$  events is expected to be much lower). The signature from double charm decays, (i.e., two muons and missing energy) is expected to yield a sensitivity<sup>39</sup> of  $\sigma_{total}^{charm} \geq 0.6 \times 10^{-31} \text{ cm}^2$ .

Figures 3 and 4 show theoretical charm production cross section for  $PP \rightarrow \text{charm}, X$  and  $\pi^+p \rightarrow \text{charm}, X$  respectively from Babcock et al.<sup>6</sup> Also shown are our estimates based on the  $\psi$  production data. The quark-antiquark contributions are shown as well as various gluon-gluon distributions. Our experiment is sensitive to all the parameterizations of the gluon distributions. The old models of Sivers<sup>36</sup> and Bourguin and Gailard<sup>37</sup> have already been ruled out by other experiments.<sup>11,12,13</sup>

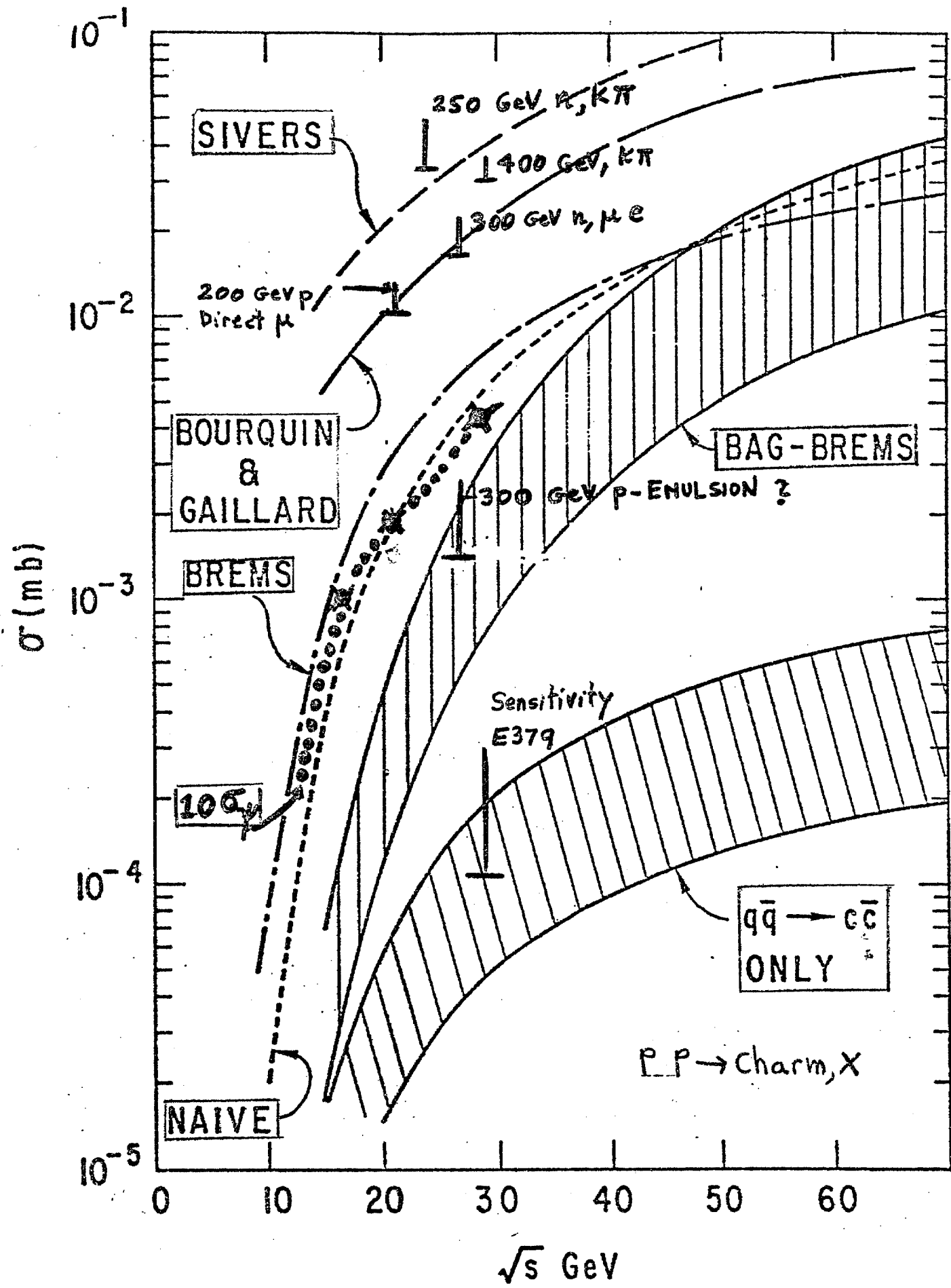


FIG. 3

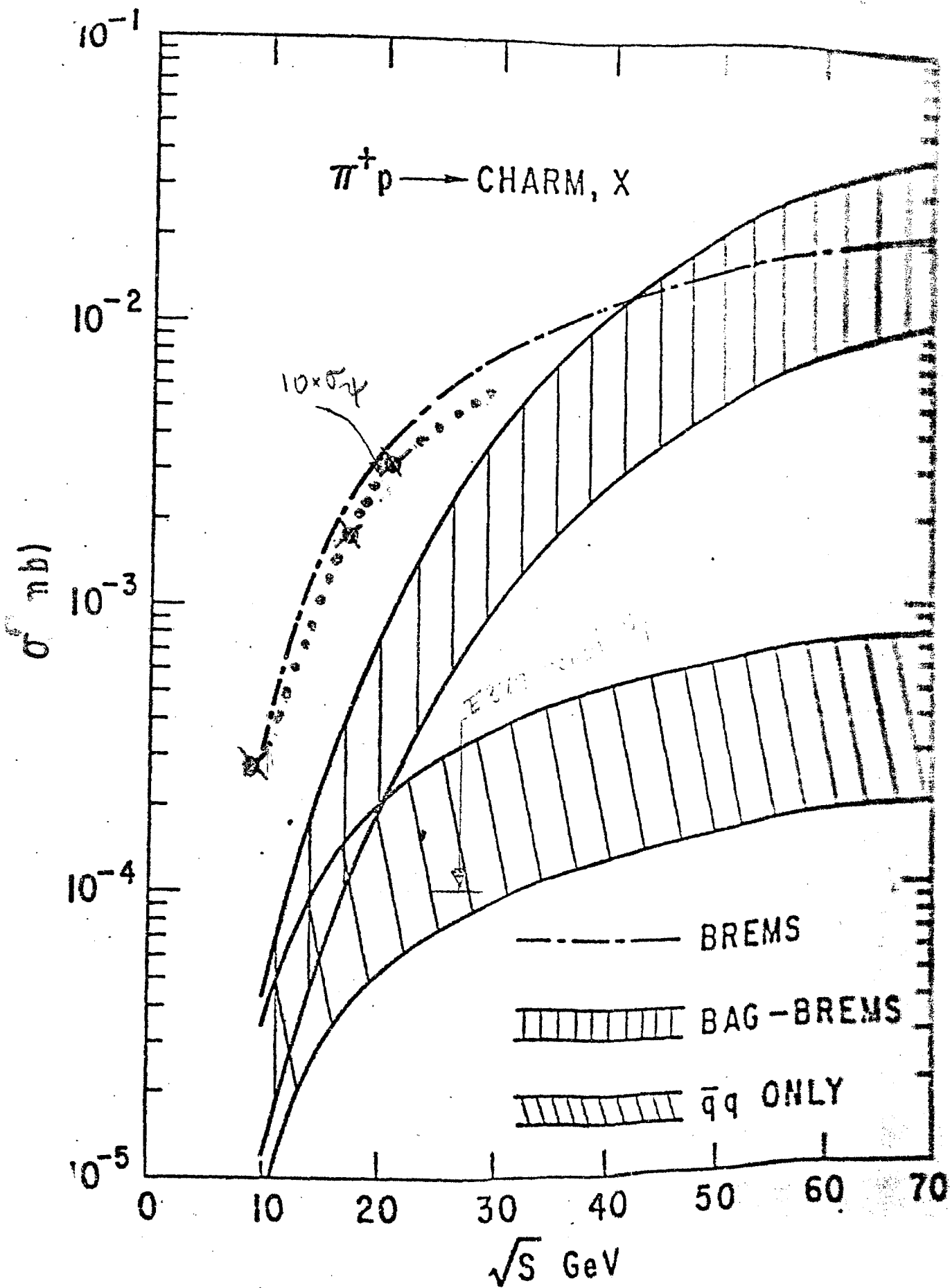


FIG. 4

Physics Goals: Low  $P_t$  Intensity Running

We plan to investigate the following physics areas in pion nucleon collisions.

1. The general  $\mu^+ \mu^-$  spectrum
2.  $J/\psi$  production and the level of  $J/\psi$  production with an extra muon (i.e. Zweig allowed production).
3. The level of direct muons originating from pairs (i.e. electromagnetic processes) as a function of  $P_t$  and  $x$ .
4. The level of direct muons produced singly (i.e. from weak decays of short lived particles) as a function of  $P_t$  and  $x$ .
5. The mean energy in final state neutrinos that are associated with the singly produced direct muons as a function of  $P_t$  and  $x$ .

At low  $P_t$ , the singly produced direct leptons are expected to be predominantly from charm production. The contribution of tau lepton production is expected to be <sup>40</sup> four orders of magnitude smaller. The distribution in  $P_t$  and  $x$  for the directly produced muons in the range  $0.0 < P_t < 1.1$  reflect the decay kinematics folded by the  $x$  and  $P_t$  distribution of production.

### Apparatus

The experiment will use the E379 setup with some modifications.

The main features of the experiment are the following:

1. Identification of neutrinos in the final state by observing "missing energy" in the reaction.
2. Very large solid angle for the observation of final state muons ( $22^\circ$  forward cone in the lab which corresponds to  $\approx 156^\circ$  in the cm) which is about 96% of  $4\pi$  in the cm.
3. Very large solid angle for the measurement of the sign and momentum of final state muons ( $10^\circ$  forward cone in the lab which is about  $130^\circ$  in the cm) which is about 80% of  $4\pi$  in the cm.
4. Energy measurement of the final state hadronic system.
5. Flexible triggering arrangement and variable density to determine meson decay contributions.
6. Good (1%) momentum tagging of incident hadrons.
7. Provisions for various incident particle with Cerenkov tagging ( $\pi^\pm, K^\pm, p, \bar{p}$ ).

The N5 beam line to Lab E will be set to transport negative particles at the highest possible momentum (250 to 300 GeV) consistent with the desired intensity. The intensity limit for reliable operation of the calorimeter is about  $10^6$ /pulse. This limit matches the intensity capabilities of the N5 beam line. Discussions with D. Theriott indicate that an intensity of about  $10^6$ /pulse is feasible at 250 GeV by targeting  $2 \times 10^{12}$  protons at the target manhole in the decay pipe. Such targeting procedure was used to provide high energy hadrons for experiments using the cyclotron magnet in the muon lab. We expect to get a similar intensity at a higher energy ( $\sim 300$  GeV) by moving the quadrupoles in enclosure 100 upstream in order to increase the solid angle.

The optimization of the beam line is presently under study by the neutrino lab. The low  $P_t$  running is limited by trigger rate and for that period we plan to run at the highest possible energy ( $E \gtrsim 300$  GeV) where  $10^5$  pions/pulse can be obtained. The Cerenkov and momentum tagging upstream of Lab E will be used.

The beam will interact in the E379 target calorimeter in lab E. Halo particles and superbuckets will be vetoed by using the existing set of trigger and veto counters.

The experiment may be viewed as a continuous calorimeter which contains a total 8.2 meters of steel along the beam direction interspersed with calorimetry counters, hodoscopes, pwc's and spark chambers. There are three major parts.

1. A fine grain calorimeter (a total of 2 meters of steel) for accurate hadron energy measurement.
2. A coarser grain calorimeter for muon identification (a total of 1.4 meters of steel).
3. The lab E toroidal magnetized calorimeter for muon sign and momentum measurement.

The fine grain calorimeter consists of 45 steel plates interspersed with scintillation counters. The first 20 plates are 1.5" thick and 30" x 30" in transverse dimensions. The last 25 plates are 2" thick and are 30" x 30" in transverse dimensions. The response of the calorimeter was measured as a function of energy between 15 and 450 GeV. The resolution varied as  $1/\sqrt{E}$  and was measured to be 3.5% at 400 GeV (see Fig. 5). The counters were calibrated with the beam line set to transport muons. An elaborate system monitored the gain of the counters throughout the run. Green LED's were used during the run to flag drastic changes in gain that had to be immediately corrected. Small gain variations were monitored using a light flasher system with fiber optics to each counter. In addition the flasher

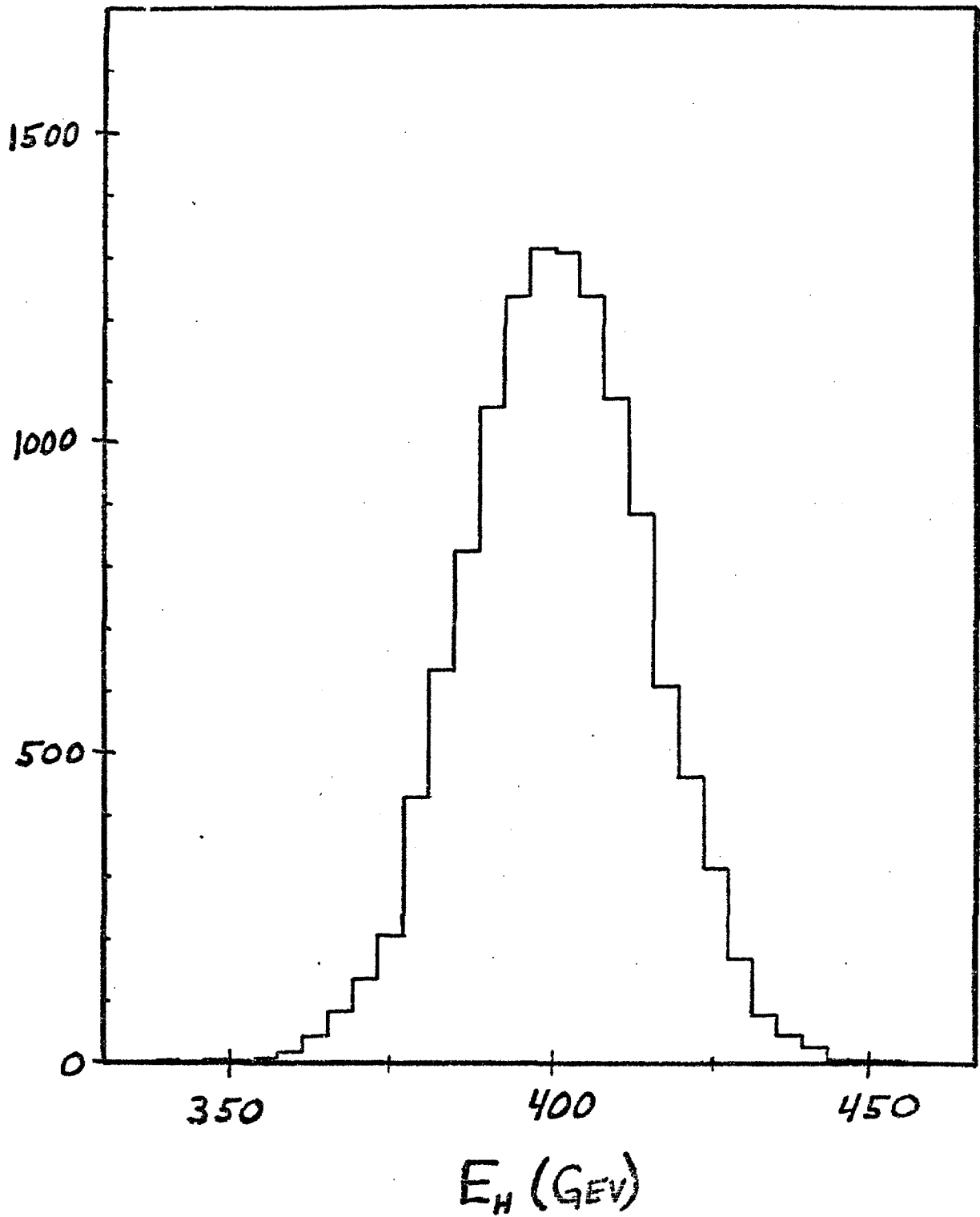


FIG. 5

The resolution of the calorimeter ( $\sigma = 3.64\%$ ) at 400 GeV.

Note the displaced zero.

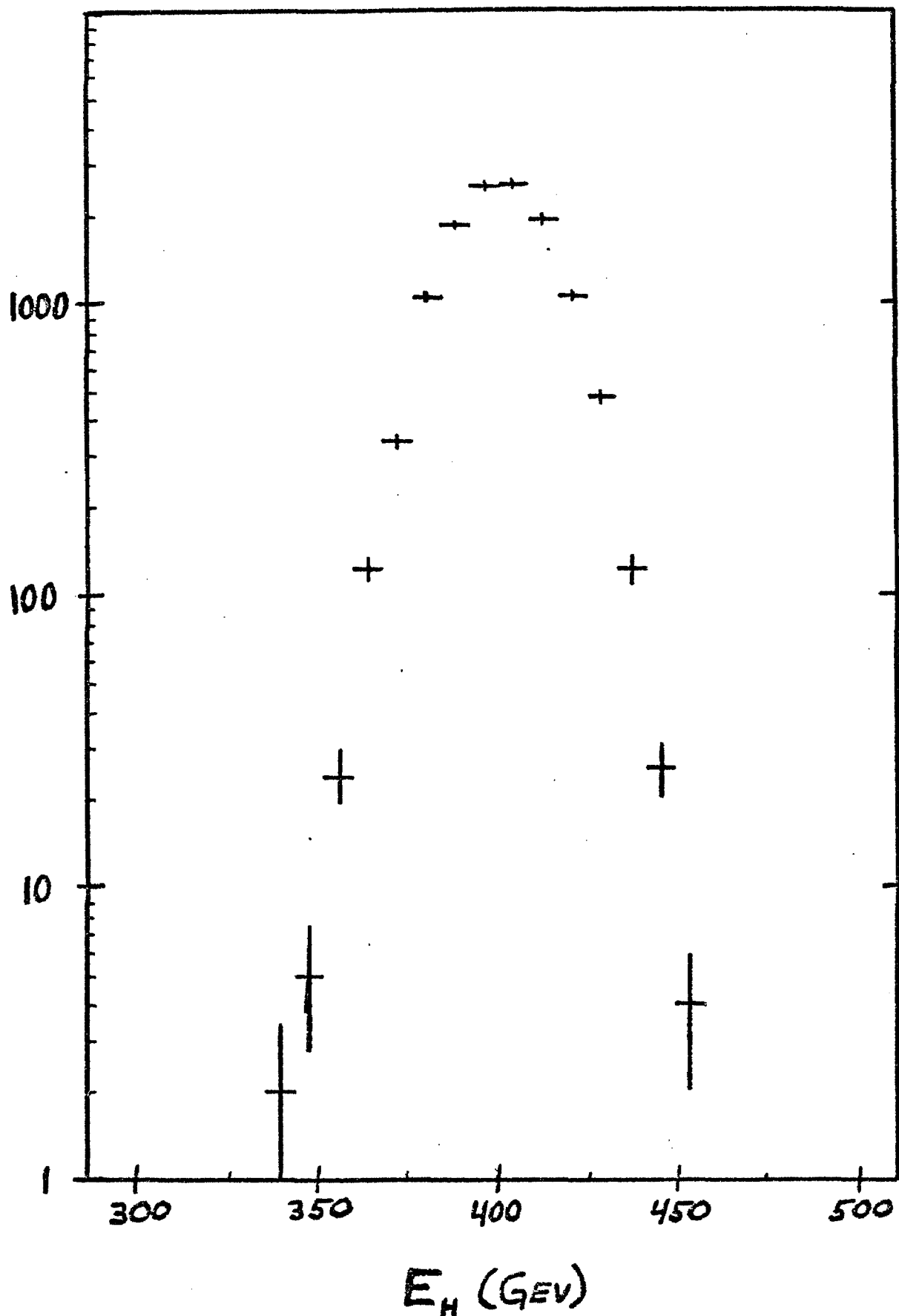


FIG. 6 The resolution of the calorimeter on semilog paper.  
It is a Gaussian with  $\sigma = 3.64\%$ . Note the displaced zero.

FIG. 7a. Calibration of the E-379 calorimeter versus incident energy (in minimum ionizing particle-inches) between 30 and 450 GeV.

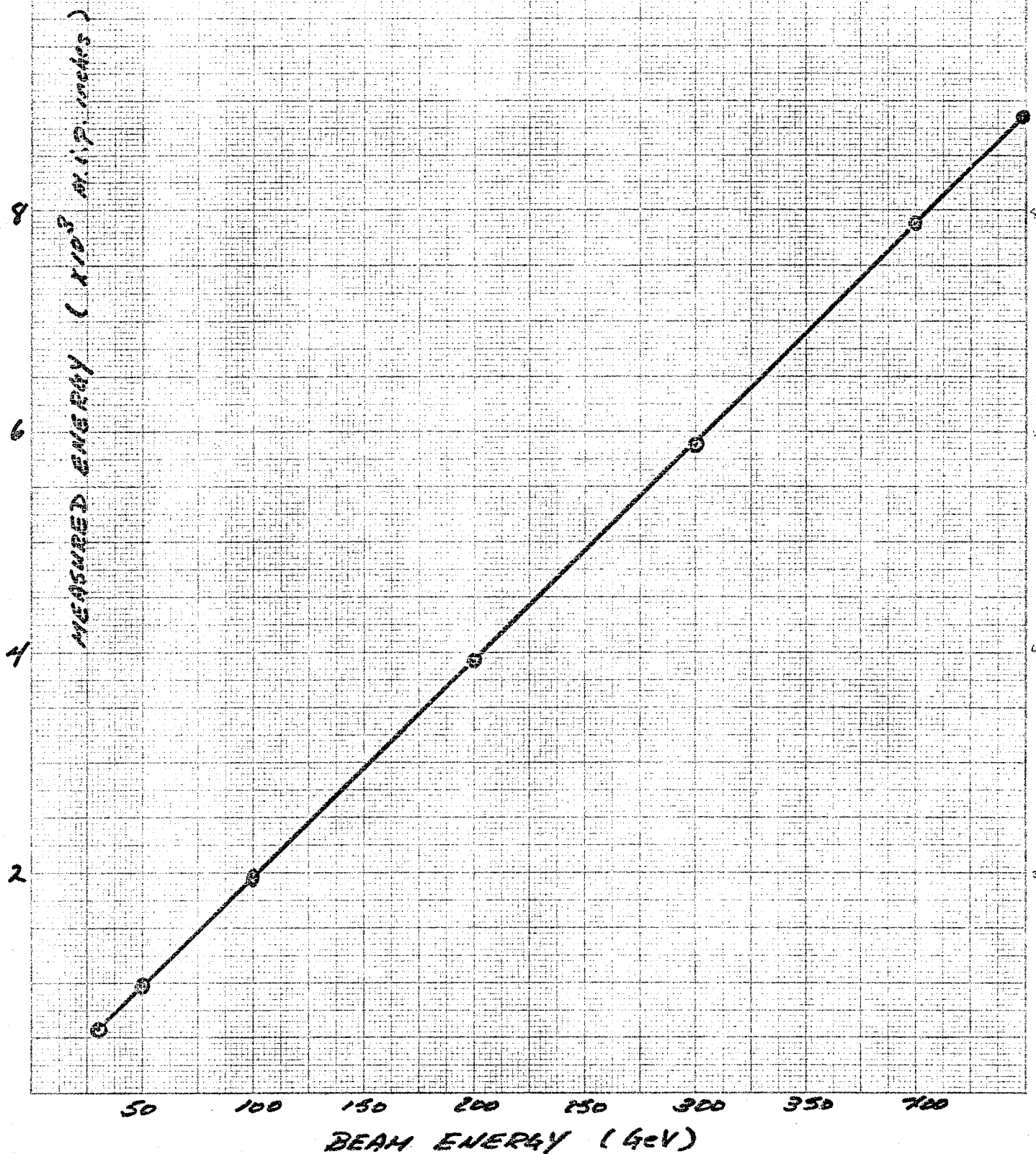
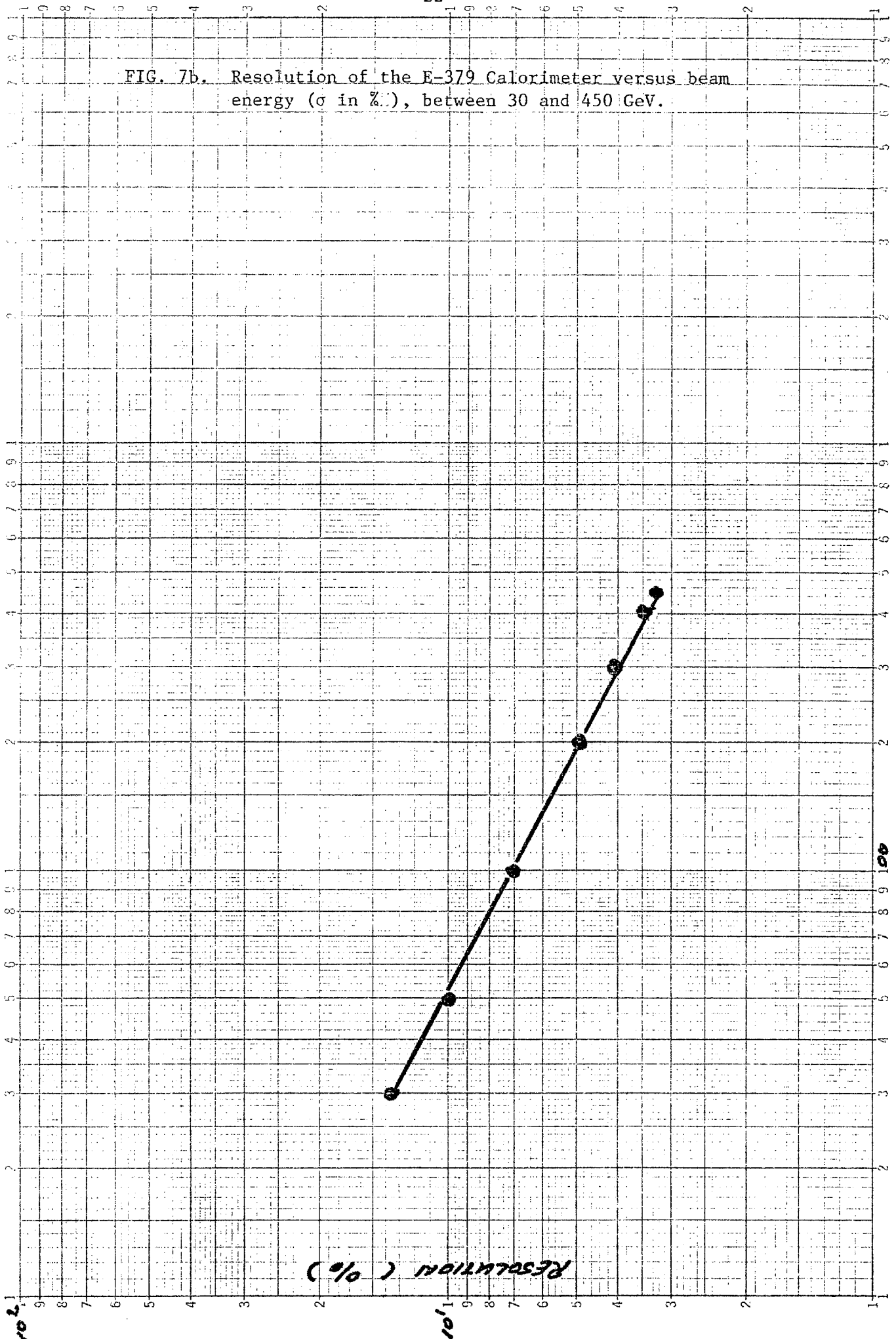


FIG. 7b. Resolution of the E-379 Calorimeter versus beam energy ( $\sigma$  in %), between 30 and 450 GeV.



light was transmitted via fiber optics to three reference phototubes placed far away from the beam. The reference tubes also viewed a sodium iodide crystal with a radioactive source which was used to monitor gain changes in the reference tubes. The flasher system was flashed and recorded within a time of 30  $\mu$ sec after each event. In order to help eliminate the instantaneous rate dependence of the phototube gains, a history of previous interactions in the calorimeters was maintained continuously and recorded with each event and with each light flasher record. We were thus able to maintain the response of the calorimeter constant in time and independent of instantaneous rate.

In the last E379 run, the fine grain calorimeter was followed by wire chambers from SLAC with capacitor-diode readout (SLAC CD chambers). These were used to measure the muon production angles (see Fig. 8). An eight inch thick steel picture frame was used to shield the outer edge of the chambers and thus help identify large angle muon. The next 1 meter of steel was a coarser grain calorimeter (10 plate each 4" thick and 48"  $\times$  48" in transverse dimensions). It was used to contain late showers and provide for forward muon identification.

Following the coarse grain calorimeter were another set of SLAC CD spark chambers that were used to determine the muon angle entering the iron toroidal spectrometer.

The muon spectrometer, which is shared with the neutrino experiment (E356) consists of three toroids. Each toroid is constructed of eight 20 cm thick magnetized iron slabs. The position and angle of a muon is determined after each 80 cm of steel by wire spark chambers with magneto restrictive readout (Caltech chambers). There are acrylic scintillation counters after every 20 cm of steel. These counters enable the toroid

RUN 381 EUT 1259

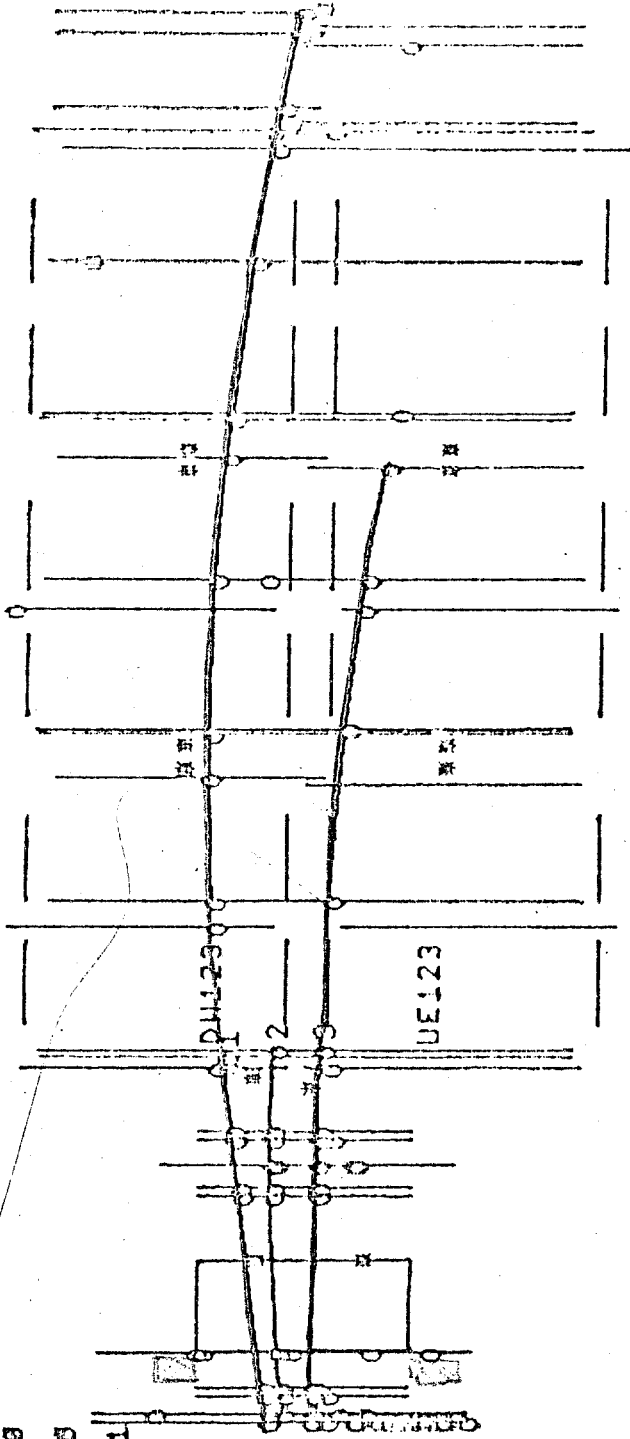
19-MAR-77 4:30: 2

ECHF 0.9

HDRN 0.0

CLK 995.1

TOP



TRIGGERS 124

SIDE

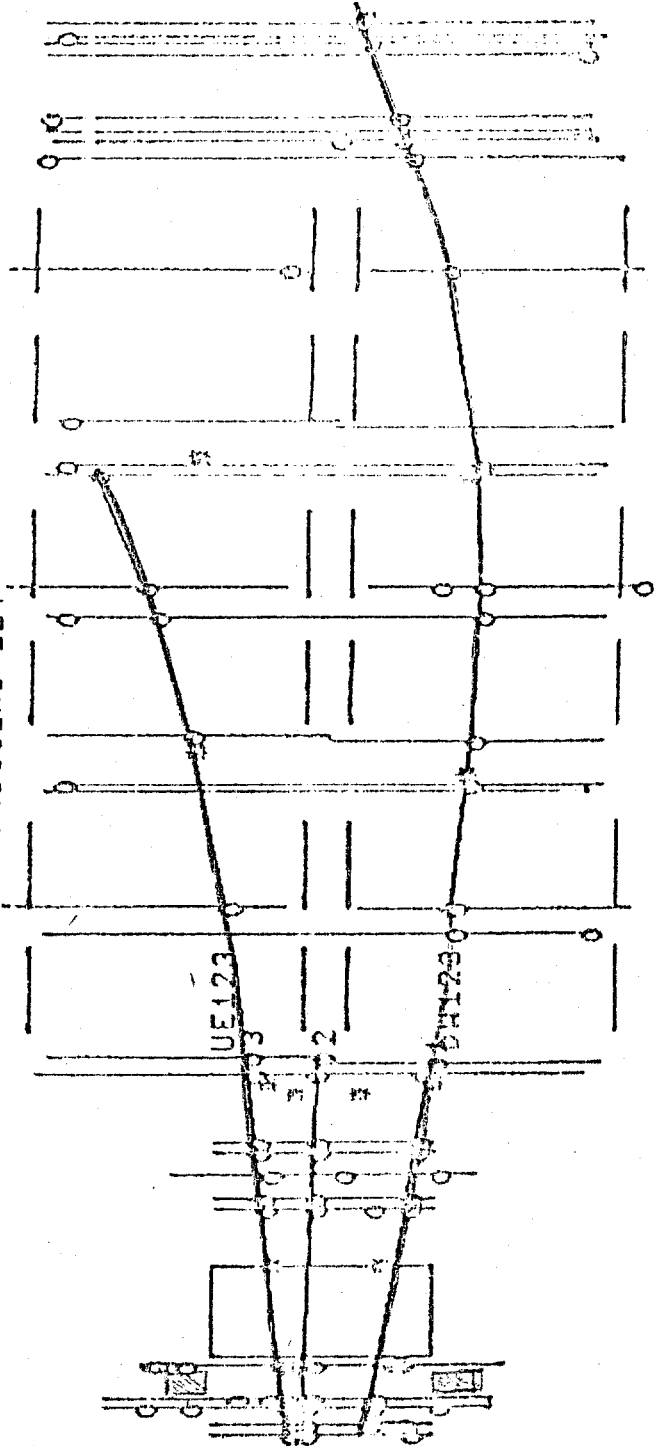
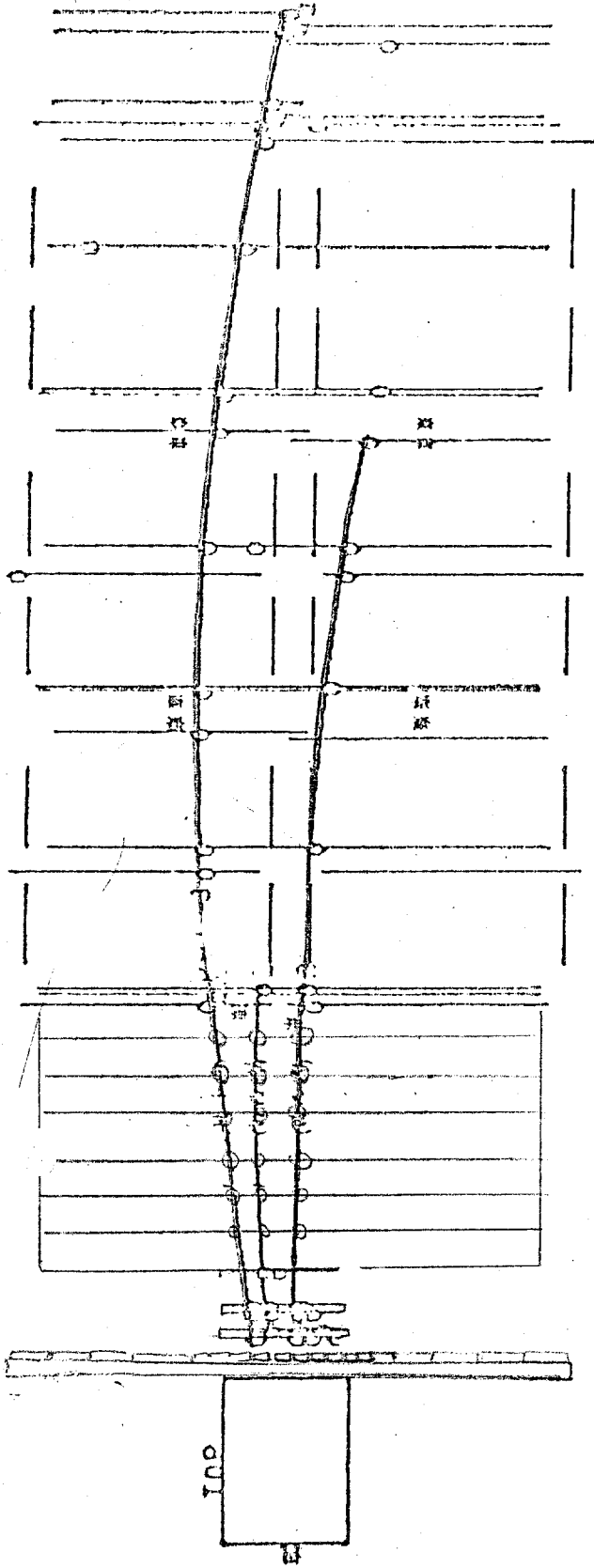


FIG. 8 Old E379 Experimental Setup

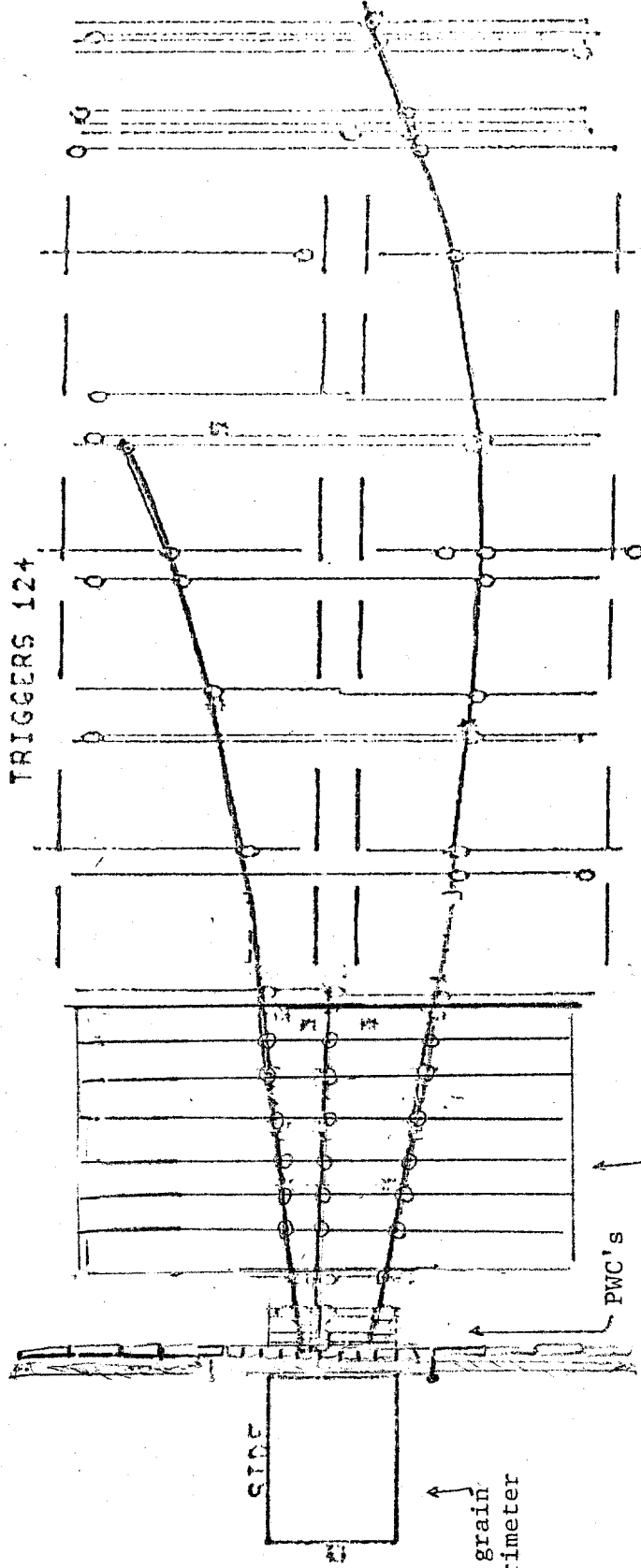
RUH 381

EVT 1259

19-MAR-77 4:30: 2



TRIGGERS 124



Fine grain Calorimeter  
 Shielded 12'x12' hodoscope  
 7 10x10' chambers  
 4 10x10' counters  
 PWC's  
 1.4 meters of steel  
 Toroid muon spectrometer  
 FIG. 9 - NEW E379 EXPERIMENTAL SETUP

system to be used as a magnetized target in the neutrino experiment. In this experiment they are used in two capacities. The first use is in the trigger. These counters are segmented into four quadrants. Therefore, by requiring muons to remain in the same quadrant and not cross into the toroid hole we can trigger on muons of high  $P_t$ . The  $P_t$  cut can be set to be as high as 1.4 GeV. The second use is in the monitoring of the rare events (~1%) where the muon interacted in the toroid steel. For such events the true energy of the muon could be mismeasured. This muon energy loss is flagged and measured by the scintillation counters. The  $P_t$  kick of the system is about 2.4 GeV with a field of about 16 kilogauss.

The momentum resolution of muons is limited by the multiple scattering in the steel. The present measured resolution is 9%. We hope to improve the resolution to 6% by better software algorithms which would place constraints on the multiple scattering since the muon track is continuously monitored throughout the steel. This way we hope to improve the mass resolution for dimuons

$$\left(\frac{\delta M}{M}\right) = \left[ \frac{1}{4} \left(\frac{\delta p_1}{p_1}\right)^2 + \frac{1}{4} \left(\frac{\delta p_2}{p_2}\right)^2 + \left(\frac{\delta \theta}{\theta}\right)^2 \right]^{1/2}. \quad \text{The observed } \psi \text{ signal in the E379}$$

proton run is shown in Fig. 10.



The new setup will make use of part of the recently constructed large 10' x 10' E356 neutrino target calorimeter as a downstream muon identifier and replace the old smaller 4' x 4' coarse grain calorimeter. The new 10' x 10' chambers in the neutrino target are interspersed between the steel and the counters and have good multitrack efficiency. The upstream CD chambers will be replaced with PWC's from a Rochester BNL experiment. The steel and the counters of the old 4' x 4' coarse grain calorimeter will be reconfigured to form a 12' x 12' hodoscope shielded by 4" of steel. The hodoscope bins at the large angles will be 1' x 2' in size. The inner 5' x 5' area will be covered by a finer hodoscope (which will also be moved from BNL) of 5" x 5" bin size. This way muon can be identified even at very large angle after only 2 meters of steel using the counters and PWC's.

One cart of the 10' x 10' neutrino target calorimeter (14 counters, 1.4 in. of steel and six 10' x 10' chambers) will be rolled over to serve as the new coarse grain calorimeter.

The sharing of a large section of the apparatus with the neutrino experiment means that there will be little interference between the two setups. Moving the toroids or neutrino carts is a rather simple operation (they move on rollers and rails) and it is routinely done to calibrate the neutrino experiment in the hadron beam. The only obstruction is the west 4' of the shielded large angle hodoscope. We will make this section easily removable such that switching from hadron to neutrino running will be simple.

### Event Rates

Since we have a totally absorbing calorimeter, the rates are directly obtained from the inelastic pion nucleon cross sections.

The  $\pi^-N$  total cross section is 24.5 mb of which 3.5 mb is elastic (in that respect using a pion beam results in a sensitivity to a somewhat lower cross section than using a proton beam for which  $\sigma_T = 42$  mb of which 7 mb is elastic). The cross sections for the reactions we wish to observe go like  $A^{1.0}$  while the total inelastic nuclear cross sections are  $^{17} 28.0 \times A^{0.75}$  mb and  $46.0 \times A^{0.69}$  mb for pions and protons respectively. Therefore, the effective inelastic cross sections per nucleon in steel are 10.4 mb and 13.2 mb for pions and protons respectively.

At an intensity of  $10^6$  pions/pulse we obtain 1 event/pulse for each  $10.4 \times 10^{-33}$  cm<sup>2</sup> of cross section. For a 15 sec cycle time we obtain 240 pulses per hour. In 100 hours = 1 week we get  $2.4 \times 10^4$  pulses. So in 100 hours we obtain

$$1 \text{ event for each } 4.3 \times 10^{-37} \text{ cm}^2$$

In the calculation of event rates we will fold in acceptance and branching ratios for the various decay modes we will be investigating.

Our spark chamber dead time is 12 msec. Therefore, we can accumulate 25 events/pulse (30% dead time). In 100 hours this corresponds to  $6 \times 10^5$  events.

We anticipate running 400 hours at low intensity ( $\approx 10^5$ /pulse) for low  $P_t$  running and 300 hours at high intensity ( $10^6$ /pulse) for the high  $P_t$  running.

Rates and background and analysis - Low  $P_t$  running.

For charm production the fraction of total production for topologies including final state muons are listed below, assuming a 12% muon decay branching ratio.<sup>41</sup> (All such topologies include also neutrinos in the final state).

<u>Muon Topology from Charm-anticharm Decays</u>	<u>Fraction of Total Production</u>
low $P_t$ $\mu^-$ + missing energy	10.6%
low $P_t$ $\mu^+$ + missing energy	10.6%
$\mu^+ \mu^-$ + missing energy	1.4%

The low  $P_t$  trigger is basically a single muon trigger requiring a certain penetration through the toroid systems and an energy deposition in the calorimeter signifying a hadron shower. In our last run with 400 GeV protons, such a trigger yielded about 30 triggers/ $0.5 \times 10^5$  protons. We expect the trigger rate to be somewhat lower for 300 GeV pions.

Using an acceptance of 20% we expect to trigger on  $4.8 \times 10^4$  charm particle muon decays in 100 hours of running. The 400 hours allows us to run a similar number of events at three density configurations. The toroid configurations are such that the toroids are off-axis to accept low  $P_t$  events.

One signal topology, i.e. the observation of singly produced muons, is a distinct signature of weak decays. Our large solid angle enables us to identify second muons unless they have such low energy ( $E_\mu < 3$  GeV) that they range out before reaching the muon hodoscope and chambers located after 2 meters of steel. The number of those misidentified dimuons can be obtained by the extrapolation of the observed dimuon distribution to determine the fraction of dimuons where the second muon had energy less than 3 GeV. Monte Carlo estimates are that the fraction is 3.5%. We expect the extrapolation to yield a determination of this fraction to better than 10% of its value. Furthermore, since the second

muon ranges out in the calorimeter, the entire energy is observed while in a true weak decay the unobserved neutrino carries energy. Thus a cut on missing energy will further discriminate against misidentified dimuons.

Also, charm decay muons are expected to have intermediate  $P_t$  ( $P_t \simeq 0.5$  GeV) while single muons originating from pairs peak around  $P_t \simeq 0$ . Therefore, elimination of events of  $P_t < 0.5$  GeV can result in additional discrimination against muons originating from pairs. Figure 10 shows the expected  $P_t$  distribution from D meson decays as calculated by Barger et al.<sup>18</sup> The  $P_t$  distribution has been calculated including a D meson production  $P_t$  distribution according to

$$\frac{dN}{dP_t^2} \propto e^{-b(m^2 + P_t^2)^{1/2}}$$

where  $m$  is the particle mass ( $m_d$  for charm) and  $b = 6 \text{ GeV}^{-1}$ . The above formula<sup>19</sup> fits all available<sup>28</sup>  $\rho$ ,  $\pi$ ,  $K$ ,  $\bar{p}$  and  $\psi$  production data.

Another background which must be measured are the single muons that originate from pion and kaon decays. These are minimized because of the high density of the calorimeter (very close to the density of steel, the counters are only 1/8" thick). The calorimeter's density can also be varied (each plate is independently movable). Data taken at different calorimeter densities is used to extract the directly produced signal. Also, since the  $\pi^+/\pi^-$  ratio differs from 1.0 (it is greater than 1 for incident protons and less than 1 for incident negative pions in some regions of  $x$ ) while charm and bottom particle production occurs in pairs, we can choose to analyze the data for which the muon sign minimizes the decay background. (For example, in the determination of the charm signal in the large  $X$  region).

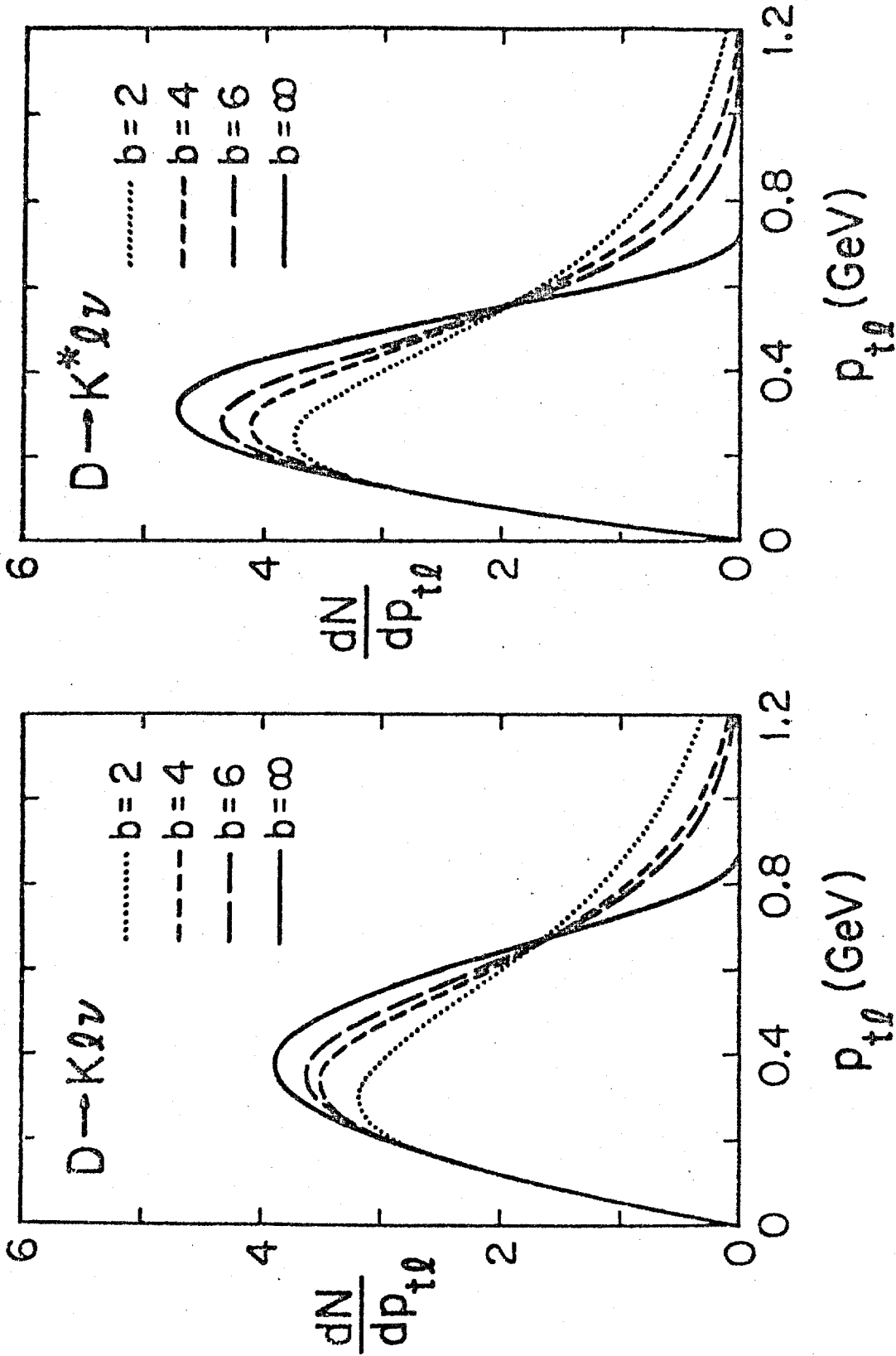


FIG. 11 - Charm particle decay final state muon  $P_t$  distributions for various production fits from Barger et.al. C00-564(1977). These fits use  $\frac{dN}{dp_t^2} \propto e^{-b(m^2 + p_t^2)^{1/2}}$  where  $m = m_D$  is the mass of the produced hadron. The value  $b = 6$  provides a best fit to  $\pi, K, \bar{P}$  and  $\psi$  production data

The second topology, i.e. dimuon events with missing energy are a signature for associated charm production. The background from  $\pi$  decay is expected to be negligible. Normal hadronic interactions in the calorimetry as well as dimuon events in the  $J/\psi$  region where no missing energy is expected will provide a monitor of the tails from zero missing energy events.

Using the above methods, we estimate that the sensitivity to detecting charm is limited to the following <sup>38,39</sup> cross sections.

- A. Using single  $\mu$  signature + missing energy <sup>38</sup>

$$\sigma_{\text{total}}(\text{charm}) \geq 0.3 \times 10^{-32} \text{ cm}^2/\text{nucleon}$$

due to the  $2\mu$  background and

$$\sigma_{\text{total}}(\text{charm}) \geq 3 \times 10^{-31} \text{ cm}^2/\text{nucleon}$$

due to the  $\pi$  and  $k$  decay backgrounds.

- B. Using the  $2\mu$  signature <sup>39</sup> + missing energy

$$\sigma_{\text{total}}(\text{charm}) \geq 0.6 \times 10^{-31} \text{ cm}^2/\text{nucleon}$$

due to the background from regular  $2\mu$  events.

Part II: High Intensity Run - High  $P_t$  and Multimuons

Introduction - Heavy Flavor Production

The recent discovery of the  $\Upsilon(9.4)$  at Fermilab<sup>4</sup> has resulted in a deluge of theoretical papers<sup>20</sup> explaining the resonance as a bound state system of a massive quark-antiquark pair of a new flavor. The quark having this new flavor has been norminally labelled bottom or beauty and the  $\Upsilon$  a  $b\bar{b}$  state. The new quark is expected to have a mass around 5.5 GeV and probably charge 1/3. It is expected that new heavy states with the quantum number of this flavor will be produced in pairs (e.g.  $b\bar{u}$ ,  $\bar{b}u$  etc.) in high energy hadron collisions. Because of the high mass of these states ( $\approx 6$  GeV) the production cross sections are expected to be low. However, if the new quantum number is conserved in strong interactions (as indicated by the narrow width of the  $\Upsilon$ ) these particles will have a large fraction of semileptonic decays. The high mass of the decaying states will yield a high  $P_t$  muon and an energetic neutrino in the final state. These massive states are also expected to be produced with flatter  $P_t$  distribution<sup>1,21</sup> and a flatter  $x$  distribution<sup>24</sup> than normal low mass states. Therefore, the  $P_t$  and energy in the laboratory of the final state leptons will be enhanced due to the  $P_t$  and  $x$  of production. The E379 apparatus with its large acceptance for final state muons and the ability to detect "missing energy" is ideally suited for the observation of such semileptonic decays.

Theory (Bottom States)

The Upsilon cross section can be used as a guide in the calculation of the total cross section for the production of bare bottom particles (they will be referred to as Bt particles in this proposal).

In analogy with charm we expect the following relation to hold<sup>7</sup>

$$\frac{\sigma_{pp \rightarrow Bt x}}{\sigma_{pp \rightarrow T x}} \approx \frac{\sigma_{pp \rightarrow \text{charm } x}}{\sigma_{pp \rightarrow \psi x}} \approx \frac{\sigma_{pp \rightarrow K \bar{K}}}{\sigma_{pp \rightarrow \phi x}} = 10 \quad (1)$$

where the  $\sigma_{K\bar{K}}/\sigma_{\phi} = 10$  is shown in figure 1.

The observed<sup>1</sup> small cross section of B  $\left. \frac{d\sigma}{dy} \right|_{y=0} = 1.8 \times 10^{-37} \text{ cm}^2/\text{nucleon}$  for the production of the T (9.5) in 400 GeV proton collisions means that the detection of B particles will be difficult. Fortunately, it is expected that the cross section in pion nucleon collisions will be greatly enhanced. Also, the x distribution is expected to be much flatter in pion than in proton reactions. For example, at 150 and 225 GeV the measured<sup>9,10</sup>  $J/\psi$  cross sections with pions are about twice that with protons, and a flatter x distribution is observed with incident pions. For the Upsilon we calculate a much larger ratio. In order to estimate the Upsilon cross section in pion collisions we use a scaling relation which relates the  $J/\psi$  production cross section at a cm energy  $\sqrt{s_1}$  to the Upsilon production cross section at cm  $\sqrt{s_2}$  such that  $m\psi/\sqrt{s_1} = mT/\sqrt{s_2}$ . A similar approach has been used by Ellis et al<sup>20</sup> to successfully account for the observed T, T' and T'' cross sections at 400 GeV proton-nucleon collisions.

Using the same procedure for incident pions we obtain the cross section times branching ratio  $\rightarrow \mu^+ \mu^-$

$$B \cdot \sigma_T(\sqrt{s}) = \frac{\Gamma(T \rightarrow \mu^+ \mu^-)}{\Gamma(\Psi \rightarrow \mu^+ \mu^-)} \left( \frac{m_\Psi}{m_T} \right)^3 B \cdot \sigma_\Psi \left( \sqrt{s'} = \frac{m_\Psi}{m_T} \sqrt{s} \right) \quad (2)$$

Using the measured<sup>8</sup>  $\Gamma(\Psi \rightarrow \mu^+ \mu^-) = 4.8 \pm 0.6$  KeV and the calculated (Ellis et al<sup>20</sup>)  $\Gamma(T \rightarrow \mu^+ \mu^-) = 0.7$  KeV we obtain

$$B \cdot \sigma_T(\sqrt{s}) = (5.2 \times 10^{-3}) \cdot B \cdot \sigma_\Psi(\sqrt{s'} = \frac{3.1}{9.4} \sqrt{s}) \quad (3)$$

Equation 3 relates the J/ψ cross section at BNL and Serpukhov to Upsilon cross sections at Fermilab.

Table 1 lists the present available data on J/ψ production in pion collisions and the predicted scaled T cross sections. We list total cross sections times branching ratio to μ<sup>+</sup>μ<sup>-</sup> in cm<sup>2</sup>/nucleon. We have assumed that σ<sub>T</sub> = 2σ (x > 0).

Energy GeV	Experiment	particle	√s	B·σ <sub>J/ψ</sub>	Scaled Energy	Scaled σ <sub>B·σ<sub>T</sub></sub>
16	BNL <sup>25</sup>	π <sup>-</sup>	5.56	3.6×10 <sup>-37</sup>	151	1.9×10 <sup>-37</sup>
22	BNL <sup>25</sup>	π <sup>-</sup>	6.49	0.3×10 <sup>-33</sup>	206	1.5×10 <sup>-36</sup>
39.5	SPS <sup>26</sup>	π <sup>-</sup>	8.61	. ×10 <sup>-33</sup>	363	1.0×10 <sup>-35</sup>
43	Serpukhov <sup>27</sup>	π <sup>-</sup>	8.98	2.2×10 <sup>-33</sup>	395	1.1×10 <sup>-35</sup>
150	FNAL <sup>9</sup>	π <sup>+</sup>	16.8	13×10 <sup>-33</sup>		
225	FNAL <sup>10</sup>	π <sup>+</sup>	20.5	20×10 <sup>-33</sup>		
225	FNAL <sup>10</sup>	π <sup>-</sup>	20.5	24×10 <sup>-33</sup>		

Table 1 - Measured J/ψ cross sections and predicted scaled Upsilon cross sections.

As can be seen in Table 1, the calculated π<sup>-</sup>p Upsilon production cross sections at 200 GeV are a factor of 10 higher than the observed

Fermilab cross sections with 400 GeV protons. There are also indications that the scaling relation tends to underestimate the higher energy cross sections and new production mechanisms may become operative at high energy. For example, recent reports<sup>28</sup> from an experiment at the ISR ( $\sqrt{s} = 62.4$  GeV) are that the  $T$  cross section is a factor of 100 bigger than at 400 GeV while the expected rise based on the  $J/\psi$  scaling curve is only a factor of 16. In addition, the Upsilon to continuum ratio is 10 to 1 as compared to 1 to 1 at 400 GeV. This indicates that the  $T$  cross section scales faster than the continuum at high energies. Also, early indications from Fermilab experiment E444 are that at 225 GeV  $\pi^-N$  collisions the cross section for  $\mu^+\mu^-$  pairs at the  $T$  region may be a factor of 9 higher ( $\sim 1.6 \times 10^{-35} \text{ cm}^2$ ) than our calculations indicate. In addition, recent theoretical calculations<sup>29</sup> of Upsilon production by pion beams, based on quark-quark and gluon-gluon fusion mechanisms, yield cross sections which are between a factor of 5 to 9 higher than our scaling model calculations (see Figure II-1).

The low energy<sup>25,26</sup>  $\psi$  production  $x$  distributions in  $\pi^-N$  collision peak at intermediate  $x$  ( $x \approx 0.3$ ) (See figure II-2). This indicates that the expected  $T$   $x$  distribution with high energy pions will be approximately flat.<sup>4</sup> The quark and gluon fusion model<sup>29</sup> also yields  $x$  distributions which are considerably flatter with incident pions than with incident protons (See figure II-3).

From the Upsilon cross sections and a calculated value (Ellis et al.<sup>20</sup>) of 3.5% for the  $T \rightarrow \mu^+\mu^-$  branching ratio and equation (1) we obtain total cross sections for bottom particle production. These are listed in table 2 for the energies 203 and 360 GeV. Listed are cross sections for three models. The scaling calculation, the model incorporating both quark-quark and gluon-gluon processes<sup>29</sup> and a model<sup>29</sup> incorporating only quark-quark processes.

Model	Negative pions 203 GeV		negative pions 360 GeV	
	$f_{pp} \sigma_Y$	$\sigma(pp \rightarrow b_t \bar{b}_t X)$	$f_{pp} \sigma_Y$	$\sigma(pp \rightarrow b_t \bar{b}_t X)$
Scaling	$0.31 \cdot 10^{-35}$	$0.9 \cdot 10^{-33}$	$1.0 \cdot 10^{-35}$	$2.9 \cdot 10^{-33}$
"q $\bar{q}$ + g g"	$0.80 \cdot 10^{-35}$	$2.3 \cdot 10^{-33}$	$1.3 \cdot 10^{-35}$	$3.8 \cdot 10^{-33}$
"q $\bar{q}$ only"	$1.20 \cdot 10^{-35}$	$3.5 \cdot 10^{-33}$	$2.0 \cdot 10^{-35}$	$5.8 \cdot 10^{-33}$

Table 2: Cross sections for upsilon and bottom particles production in  $\text{cm}^2/\text{nucleon}$  for the three models discussed in the text. The reason this "q  $\bar{q}$  only" model yields higher cross sections is because this model is normalized to the observed upsilon cross section for 400 GeV protons. If only  $\bar{q}$  q processes contribute, then the pion cross sections will be much larger because of the larger antiquark content of the pion.

We will take the scaling model cross sections as lower limits in our rate calculations. We will take the results of the "q  $\bar{q}$  + g g" model as the rates we expect to get. The cross sections for the "q  $\bar{q}$  only" model will be viewed as optimistic numbers.

We note that the calculated charm production cross sections (see Part I) are a factor of 1000 larger than the cross section for bottom particle production. Separation of the two contributions means that a good measurement of the low  $P_t$  muons originating from charm decays is necessary in order to know the charm production contribution to singly produced high  $P_t$  muons. We will address this question in a later section.

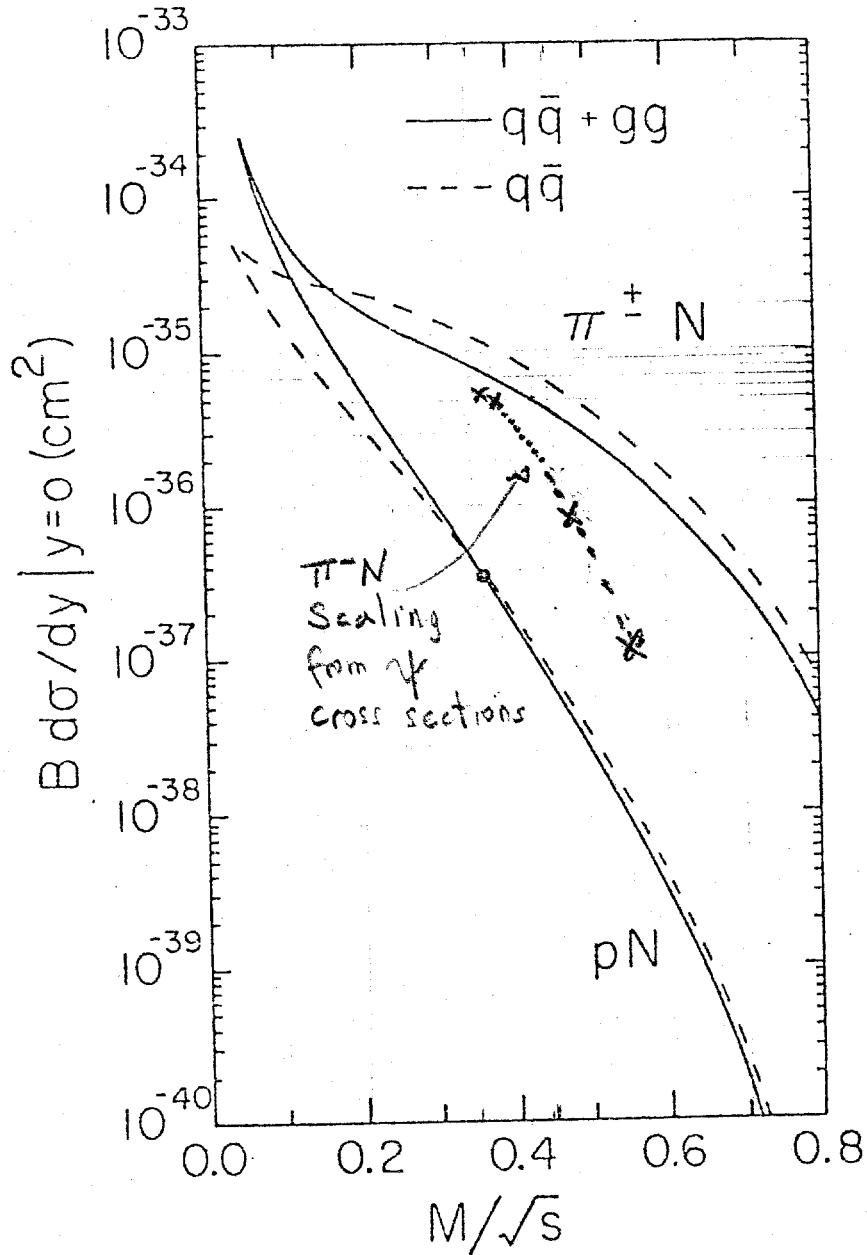


FIG. II-1

Calculated cross sections for  $\pi$ -N and pN Upsilon productions from quark and gluon fission models of J. F. Owens and E. Reya "Hadron T Production, Parton distributions and QCD" FSU HEP 770920 (Oct. 1977) unpublished. The pN data point is from S. W. Herb et al., Phys. Rev. Lett. 39, 252 (1977). The  $\pi$ -N points are based on our own calculation of scaling the low energy  $\pi N \rightarrow \psi$  cross section (we have assumed  $\left. \frac{d\sigma}{dy} \right|_{y=0} \approx \sigma_{\text{total}}/2$ ).

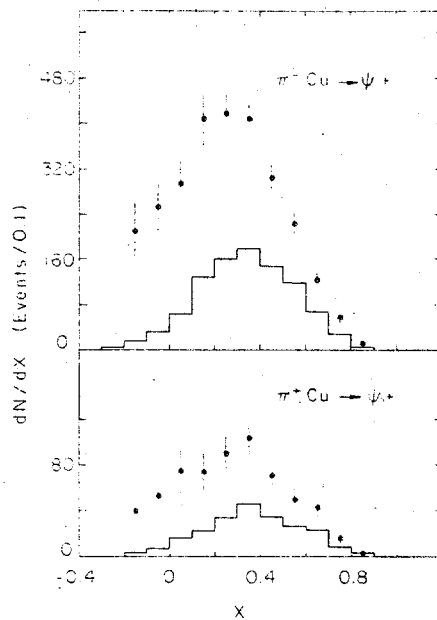


Fig. 3.  $dN/dx$  distributions for  $\mu^+\mu^-$  pairs of effective mass  $2.7 < M_{\mu\mu} < 3.5 \text{ GeV}/c^2$  (a) for  $\pi^-$  beam (b) for  $\pi^+$  beam. The histograms show the raw data. The points, with statistical errors only, represent the data corrected for acceptance.

FIG. II-2

X distribution of  $\pi N \rightarrow \psi X$  for 39.5 GeV pions from M. J. Corden et al. Phys. Lett. 68B, 96 (1977). We expect these to reflect high energy upsilon X distribution if the scaling model is valid.

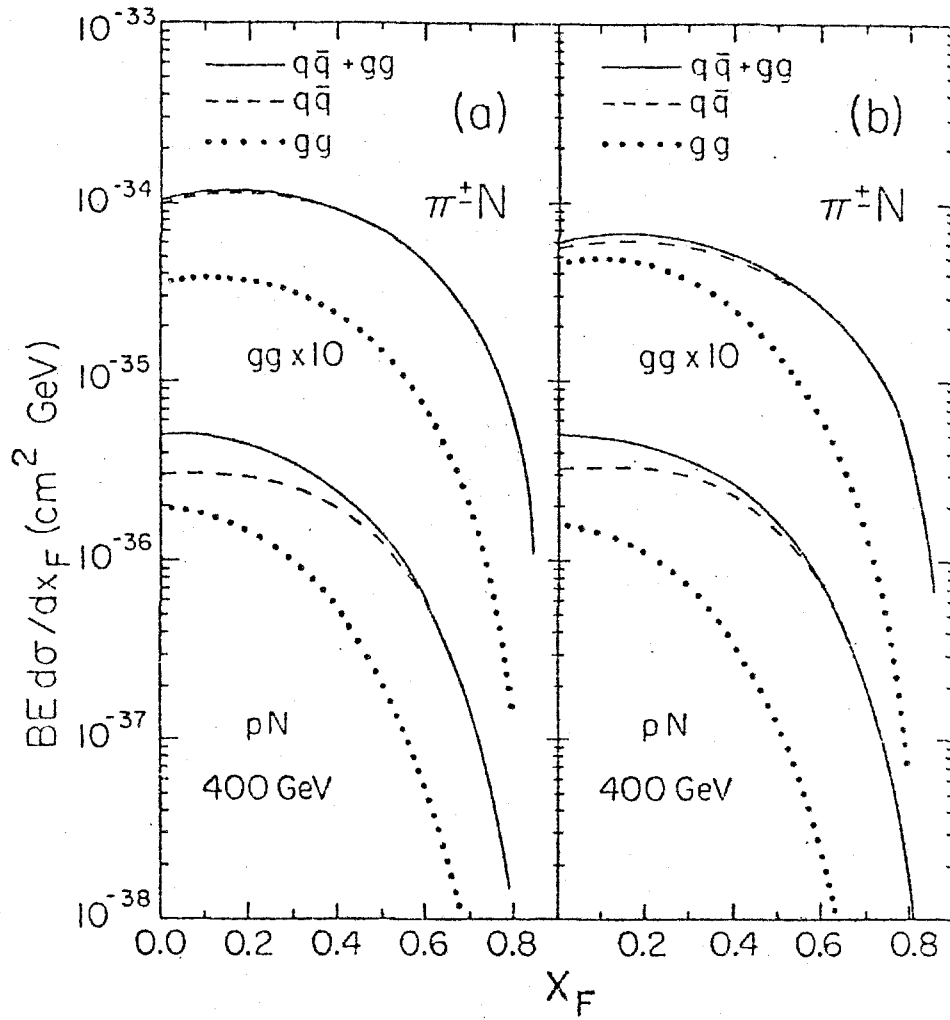


FIG. II-3

Calculated X distribution for upsilon production at 400 GeV from the quark and fusion model of J. F. Owens and E. Reya "Hadron T production, Parton Distribution and QCD", FSU-HEP-770920 (1977) unpublished.

Physics Goals - High  $P_t$  Running

We list the physics goals that are anticipated for a long high  $P_t$  run. The preliminary short run could only achieve a fraction of these goals.

1. The general  $\mu^+\mu^-$  spectrum of high mass ( $m_\mu \geq 2 \text{ GeV}$ ).
2.  $J/\psi$  production of the level of  $J/\psi$  production with an extra muon (e.e. Zweig allowed production).
3. The level of direct muons at high  $P_t$  originating from pairs (i.e. electromagnetic).
4. The level of high  $P_t$  muons produced singly (i.e. from weak decay of massive particles).
5. The missing energy associated with singly produced muons at high  $P_t$ .
6. Separation of the directly produced single muon signal into components resulting from decays of particles of intermediate mass (i.e. charm, tau leptons) and the components resulting from decays of high mass states (i.e. top, bottom). This will be done using the  $s$ ,  $P_t$ , and missing energy distribution of the events.
7.  $T$  particle production.
8. MultimMuon events and like sign dimuon events (i.e.  $\mu^-\mu^-$  and  $\mu^+\mu^+$ ). Like sign dimuon events with a lot of missing energy may be a good signature for bottom particle production. (See next section.)
9. Top particle production. If the  $T'$  is a  $t\bar{t}$  state<sup>30</sup> instead of a radial excitation of the  $T$ , then we expect the calculated rates to be a factor of two larger due to the opening of this other channel for production of heavy states.

Event Topologies and Rates

We will use the case of bottom particle production as an example for the event topologies and rates that we will be studying. Using our calculated cross sections and the branching ratios evaluated in Appendix A, we obtain the following number of events occurring in 1000 hours of running. All bottom particle muon decay topologies include neutrinos in the final state. The number of events is listed for the three models (i.e. scaling,  $q\bar{q} + gg$  and  $q\bar{q}$  only).

topology	fraction of total production	events with 206 GeV $\pi^-$ beam			events with 360 GeV $\pi^-$ beam		
		scaling, $q\bar{q}+gg$ , $q\bar{q}$ only			scaling, $q\bar{q}+gg$ , $q\bar{q}$ only		
$B_t \bar{B}_t$ decays							
high $P_t \mu^+$	7.1%	748	3861	5791	4820	6266	9640
high $P_t \mu^-$	7.1%	748	3861	5791	4820	6266	9640
medium $P_t \mu^+$	11%	1259	5982	8973	7468	9708	14936
medium $P_t \mu^-$	11%	1259	5982	8973	7468	9708	14936
$\mu^+ \mu^-$	8.4%	885	4568	685	5703	7414	14828
$\mu^- \mu^-$	1.6%	169	670	1305	1086	1412	2824
$\mu^+ \mu^+$	1.6%	169	670	1305	1086	1412	2824
$3\mu$	2%	211	1089	1634	1357	1764	3528
$4\mu$	0.1%	11	54	81	68	88	136
$T \rightarrow \mu^+ \mu^-$	3.5%	37	188	283	234	304	468

The above numbers should be multiplied by the trigger efficiencies and acceptance. These are discussed in the triggers and backgrounds and acceptance sections.

Triggers, Backgrounds and Analysis - high  $P_t$  Running

Triggering on high  $P_t$  muons is relatively easy. The toroid spectrometer focusses low  $P_t$  muons into the toroid axis. The requirement that muons traverse a certain longitudinal distance before they cross the axis corresponds directly to a minimum  $P_t$  requirement. Defocussing muons are rejected in the trigger by requiring counters of the same solid angle to fire. These counters are located in front and behind the toroid. Defocussing muons miss the correct rear counter. The  $P_t$  cut can be varied up to 1.4 GeV (corresponding to the location of the furthest downstream counter we have in the system). In the E-379 run with 400 GeV protons we could easily run with a  $P_t$  cut as low as 0.8 to 1.0 GeV and a trigger rate of 20 per  $10^6$  protons. However, the ability to increase the  $P_t$  cut is always there if the trigger with 250 GeV pions turns out to be larger (though we expect it to be lower). As a matter of fact, we expect the trigger to be much cleaner now because all acrylic counters in the toroids are presently installed. In the last E-379 run a large fraction of the acrylic counters were missing and some very low  $P_t$  muons with S trajectories could trigger.

The small hole in the toroid (10" in diameter) prevents the measurement of the very forward low  $P_t$  muon spectrum. In order to measure the complete muon production over all angles we use the low  $P_t$  data taken with the toroids off-axis.

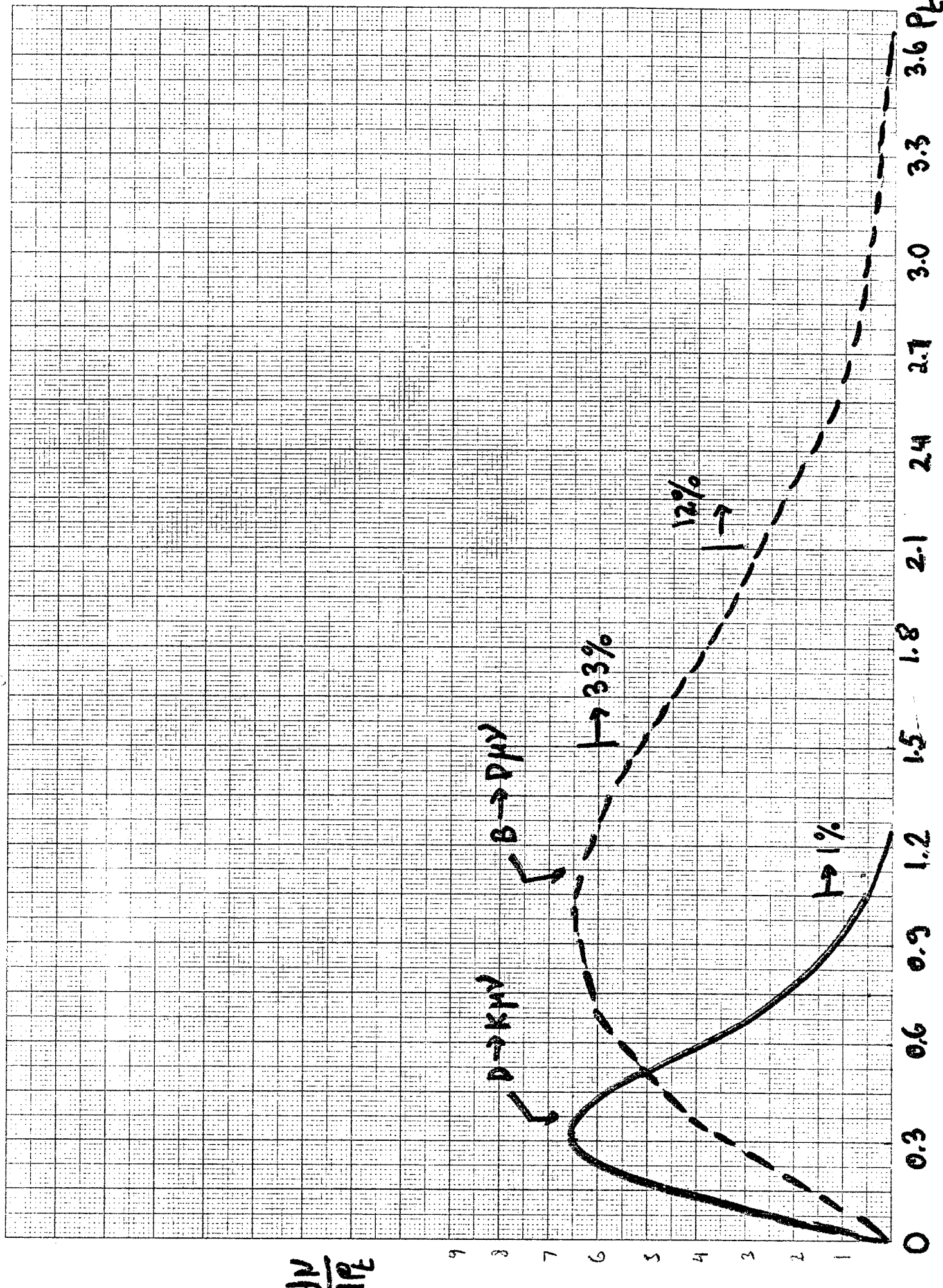
For study of high  $P_t$  singly produced muons, the toroid hole may even be advantageous. Assymmetric decays of dimuons that lead to low energy second muons and thus may be misidentified typically have the forward muon go through the hole. In order to yield a high  $P_t$  muon ( $P_t \geq 1.5$  GeV) as well as to have a large angle assymmetric decay the dimuon mass must be large ( $m_{\mu\mu} \geq 2 \times 1.5/\sin(156^\circ) \simeq 7.4$  GeV). This is because although lower mass pairs may be produced

with a high  $P_t$ , the pair velocity in the center of mass is small and the production  $P_t$  does not add much to the final  $P_t$  of the decay muons. Thus, because of the large required mass, the number of such pairs is expected to be small. Furthermore, the high  $P_t$  muon from the pair goes forward near the region of the hole. So by the elimination of events in the neighborhood of the hole we can greatly discriminate against such events with only a small ( $\sim 2.5\%$  of  $4\pi$ ) additional loss of solid angle.

Since the charm production cross sections are about 1000 times larger than the cross sections for bottom particle production, the number of observed events from charm decay is expected to be large. The spectrum of directly produced muons will contain both muons from charm and muons from bottom particle production. However, as can be seen in Figure II-4, a very small fraction of muons originating from charm decays have  $P_t$  greater than 1.0 GeV ( $\cong 1\%$ ) and less than 0.1% have  $P_t$  greater than 1.2 GeV. We have used the  $D \rightarrow K\mu\nu$  decay distribution to obtain the distribution<sup>35</sup> for the bottom particle decay  $B_t \rightarrow D\mu\nu$ . A  $P_t$  cut of 1.5 GeV would eliminate almost all muons from charm decays while retaining 33% of the muons originating from bottom particle decays. Even a  $P_t$  cut as high as 2.1 GeV would retain 12% of the muons originating from bottom particle decays.

An additional signature would be the larger missing energy associated with bottom decays. As a matter of fact, the analysis of bottom decays may be easier than the analysis of the charm signal. For charm, the missing energy in the neutrino (assuming  $P_t$  of 0.5 GeV) is  $0.5 \times \gamma = 0.5 \times 11.6 = 6$  GeV for 250 GeV pions at  $x = 0$  and larger at larger  $x$ . Our  $\frac{\text{missing energy}}{\text{resolution}}$  at 250 GeV is 11 GeV, therefore the missing energy for charm events is determined on a statistical basis for the large number of charm decays. For bottom particle production the missing energy is a factor of 3 larger and therefore the missing energy may be observed on an event by event basis for a large fraction of the bottom decay events.

Figure 10



If bottom particles preferentially decay to charmed particles (see Appendix A) then like sign dimuon events such as  $\mu^- \mu^-$  and  $\mu^+ \mu^+$  events with a large missing energy would occur. The ratio of such events to the single muon decay events would indicate if the decay of the bottom to charm is dominant. Double pion and kaon decays as well as charm decays accompanied by a decay of high  $P_t$  pion or kaon would constitute the background for such events. The decay backgrounds would be determined by using the data at the various densities.

The multimMuon events will be studied in the high intensity run via an independent trigger. The large number of counters in the experiment allows us great flexibility in the trigger. In addition to the muon hodoscope the rest of the counters in the system can discriminate between 1,2 or more muons on the basis of pulse height. We can thus trigger on low  $P_t$  multimMuon events by tuning the trigger to require 2,3 or 4 muons anywhere in the apparatus. The pulse height method was used in the previous proton data run. In that run it was found that requiring three muons to penetrate one toroid (such that all their momenta are measured) results in a very low trigger rate at  $10^6$  protons/pulse. Therefore, a high  $P_t$  muon is *not* required to be in the multimMuon trigger.

MultimMuon events such as  $J/\psi$  production with an extra muon are easily recognized. The  $\pi$ , K decay background is directly determined. In this study the third muon need only be identified but not necessarily measured. Our muon identification capability which covers 96% of  $4\pi$  for muons with  $P > 3$  GeV would enable us to find muons from charm decay. The charmed particles produced in association with the  $\psi$  are expected to be produced at  $X=0$  and therefore lead to very low energy

muons ( $E < 10$  GeV). Our sensitivity is at least a factor of 10 better than other experiments<sup>31</sup> because of our larger acceptance, ability to detect lower energy muons ( $E > 3$  GeV vs.  $E > 7$  GeV in other<sup>31</sup> experiments) and our shorter decay path (20 cm vs 160 cm).

The background for high mass 3 and 4 muon events with missing energy (as expected from bottom particle decay topologies) is expected to be small. No such events have been observed in a recent experiment<sup>31</sup> which collected about 900 pion induced  $\psi \rightarrow \mu^+ \mu^-$  events at 225 GeV. This means that the multimMuon cross section with pions is less than  $10^{-3}$  of the  $\pi N \rightarrow \psi \rightarrow 2\mu$  production cross section.

In addition to 4 muon events from bottom particle decays, there may be a small signal<sup>32</sup> of 4 muon events with no missing energy such as charm related processes.

$$\chi_c \rightarrow \gamma_v \psi \rightarrow 4\mu$$

$$\eta_c \rightarrow \gamma_v \gamma_v \rightarrow 4\mu$$

$$\eta_c \rightarrow \phi \phi \rightarrow 4\mu$$

and bottom quark related processes

$$\eta_b \rightarrow \psi \psi \rightarrow 4\mu$$

and other  $\eta_b, \chi_b \rightarrow 4\mu$  decays.

The observation of such decays will be very interesting. More likely though, the cross sections are so small<sup>33</sup> such that if any events are observed, they could easily be differentiated from the  $4\mu$  events with missing energy. Any other unexpected multimMuon events with or without missing energy would be exciting new physics.

### Acceptance and Efficiencies

In this section we discuss the acceptance and efficiencies and present the expected number of events with those factors folded in.

There is an overall 50% loss from the following combination of sources. The 12 msec spark chamber dead time leads to a 30% loss at 25 events/pulse. We expect to lose 10% of the events such as those that have late hadron showers, superbuckets, bad spill or halo particles. The general loss from experimenter equipment down time, time to change tapes, change calorimeter densities etc., is estimated at 20%.

The trigger includes almost all the forward hemisphere in the cm and part of the back hemisphere. We use an acceptance of  $50\% \frac{of}{\wedge} 4\pi$  as guide (see Appendix B).

Triggers requiring a high  $P_t$  muon have another efficiency factor. As discussed earlier (see fig. 10) 33% of the  $B_t \rightarrow D\mu\nu$  muons have  $P_t > 1.5$  Gev and 12% have  $P_t > 2.1$  GeV. The resulting number of events in 1000 hours of running is listed in the table below for three different production models. The toroids are assumed to be set to focus positive muons.

As can be seen from the table, a time larger than 1000 hrs. is necessary for the measurement, as the time needs to be divided between 3 density configurations.

Topology and fraction of  $4\pi$  acceptance (There is an additional 0.50 factor due to dead time and down time)

1000 hours: Detected events, all efficiencies dead time, down time and acceptance cuts included.

		203 GeV $\pi^-$			360 GeV $\pi^-$			
		scaling	$q\bar{q} + gg$	$q\bar{q}$ only	scaling	$q\bar{q} + gg$	$q\bar{q}$ only	
B, B <sub>t</sub> decays:								
single $\mu^+$	$p_t > 1.5$ GeV	$0.5 \times 0.30$	56	290	434	362	470	723
	$p_t > 2.1$ GeV	$0.5 \times 0.12$	23	116	174	145	188	289
$\mu^+, \mu^-$	( $p_t > 1.5$ GeV)	$0.8 \times 0.5 \times 0.3$	53	274	411	342	445	890
$\mu^+, \mu^-$	( $p_t > 2.1$ GeV)	$0.8 \times 0.5 \times 0.12$	21	110	164	137	178	356
$\mu^+, \mu^+$	( $p_t > 1.5$ GeV)	$0.8 \times 0.5 \times 0.3$	10	40	78	65	85	169
$\mu^+, \mu^+$	( $p_t > 2.1$ GeV)	$0.8 \times 0.5 \times 0.12$	4	16	31	26	34	68
$3\mu$		$\sim (0.8)^3$	52	279	418	347	452	903
$4\mu$		$\sim (0.8)^4$	+2	11	17	14	18	28
$\gamma \rightarrow \mu^+ \mu^-$		$\sim 0.5$	9	47	71	59	76	117

Summary: High Intensity Running

The feasibility of detecting bottom states looks promising. However, a long dedicated run in the ballpark of 1600 hours appears necessary. The success of such a run hinges on the level of signal and the various backgrounds. The backgrounds are primarily pion and kaon decays and misidentification of two muon events. Our calculations of the backgrounds indicate that using the available experimental tools (such as density comparison, second muon identifier, missing energy and  $P_t$  distributions), we will obtain a measured cross section at the 2 standard deviations level after background subtractions. Since the levels of cross sections and backgrounds are uncertain by a factor of 4, it means that under optimistic assumptions a good measurement is feasible while in the pessimistic case, only a limit is feasible.

The preliminary 300 hour run will yield valuable information about the background and yield cross section limits within a factor of 5 of the anticipated level of  $\sigma_{\text{total}} \cdot B(\mu\nu X) \simeq 1.4 \times 10^{-34} \text{ cm}^2/\text{nucleon}$ .

The above results are based on the assumption that the only source of high  $P_t$  singly produced direct leptons is the semileptonic decay of bottom states. If other sources exist then such states may even be seen in the short preliminary run. For example, a recent article by Nieh<sup>34</sup> has suggested that the two body decays  $B \rightarrow \mu\nu$  of the  $1^-$  bottom states may be important. If that is the case, we have a good chance of detecting such decays because they yield higher  $P_t$  muons and a larger missing energy than the three body decays. The background at the higher values of  $P_t$  are much smaller.

We also expect the high  $P_t$  run to yield the expected "bread and butter" physics of  $PN \rightarrow \mu X$  experiment. In our case it means determining whether directly produced high  $P_t$  muons come from pairs at the 99% level, and measuring  $J/\psi$  cross section, X distributions and  $J/\psi$  production with an extra muon, and the general  $2\mu$  high mass spectrum.

References: Parts I and II

1. G. Goldhaber et al., Phys. Rev. Lett 37, 255 (1976); I. Peruzzi et al, Phys. Rev. Lett. 37, 569 (1976).
2. B. Knapp et al., Phys. Rev. Lett 37, 882 (1976); D. O. Caldwell et al., Fermilab Preprint; W. Chen, invited talk at the 1977 International Symposium on Lepton and Photon Interactions at High Energies, August 25-31, 1977, Hamburg, Germany; D. W. G. S. Leith In "Electromagnetic Interactions of Hadrons", A. Donnachie and G. Show eds., Plenum Press.
3. C. Baltay, private communication; B. C. Barish et al., Phys. Rev. Lett. 39, 981 (1977); A. Benvenuti et al., Phys. Rev. Lett. 34, 419 (1975); C. Baltay et al., Phys. Rev. Lett 39, 62 (1977), and E. Z. Gazzoli, et al. Phys. Rev. Lett. 34, 1125 (1975).
4. S. W. Herb et al., Phys. Rev. Lett. 39, 252 (1977); W. R. Innes et al., Phys. Rev. Lett. 39, 1240 (1977).
5. Fermilab Proposal E-379, Search for Short Lived States Decaying Weakly via Leptonic Modes, Caltech/Stanford Proposal, February 1975 (S. Wojcicki, Spokesperson).
6. John Babcock, Dennis Sivers, Stephen Wolfram, "QCP Estimates for Heavy Particle Production" ANL-HEP-77-68 (Oct. 1977).
7. F. Halzen, "Probing the New Particles with Hadron Beams", in Proceedings of the International Conference on Production of Particles with New Quantum Numbers, pg. 123; D. B. Cline, J. J. Kolonko, editors, Madison, Wisconsin, (1976).
8. G. J. Feldman and M. L. Perl, Phys. Reports 336, (Oct. 1977).
9. K. J. Anderson et al., Phys. Rev. Lett. 37, 799 (1976).
10. J. G. Branson et al., Phys. Rev. Lett. 38, 1331 (1977).

11. M. A. Abolins et al., "Search for Charm Production in Neutron Interactions near 250 GeV/c". They quote a limit of  $\sigma \cdot \text{BR} = 300$  nb/nucleon in the  $K\pi$  channel of the  $D(1870)$  for  $x > 0$ . Using the branching ratio of  $2.2 \pm 0.5\%$  (see ref. 14) we obtain  $\sigma_{D\bar{D}} < 28\mu\text{b}$ .
12. W. R. Ditzler et al., Phys. Lett. 71B, 451 (1977). They quote  $B_{K\pi} \left. \frac{d\sigma}{dy} \right|_{y=0.4} < 290$  nb/nucleon. Using  $\sigma_T \approx 2 \frac{d\sigma}{dy}$  and  $\text{BR}(D1870 K\pi) = 2.2\%$  we get  $\sigma_{D\bar{D}} < 26\mu\text{b}$ .
13. D. Spelbring et al., "Search for  $D^0(1865)$  Mesons Produced in Association with Prompt Leptons in Hadronic Interactions", Fermilab-Pub-77/63-Exp.(1977) gives  $\sigma_{D\bar{D}} < 44$   $\mu\text{b}/\text{nucleon}$  for 300 GeV neutrons; R. Lipton et al., "Search for Leptons Produced in Association with Prompt Muons in Hadronic Interactions" gives  $\sigma_{\text{charm}} < 15$   $\mu\text{b}/\text{nucleon}$ , Fermilab-Pub-77/64-Exp.(1977).
14. P. A. Rapidis et al., Phys. Rev. Lett. 39, 526 (1977); G. J. Feldman, "Properties of the D Mesons" SLAC Pub. 2000 (Aug. 1977).
15. G. Coremans-Bertrand et al., Phys. Lett. 65B, 480 (1976).
16. J. G. Branson et al., Phys. Rev. Lett. 38, 457 (1977).
17. W. Busza in Proceedings of the Seventh International Colloquium on Multiparticle Production, Tutzing, Germany, 1976, edited by J. Benecke et al., Max Planck Institute, Munich, Germany (1976).
18. V. Barger, T. Gottschalk and R. J. N. Phillips, "Multihadron Semileptonic Decays of Charmed Mesons", C00-881-564 (Feb. 1977) (unpublished).
19. J. D. Bjorken, SLAC Report 191 (1975); for other fits of production  $P_t$  distributions see M. Bourquin and J. M. Gaillard, Phys. Lett. 59B, 191 (1975), Nucl. Phys. B114, 334 (1976); D. Sivers, Nucl. Phys. B114, 45 (1976).
20. J. Ellis, M. K. Gaillard, D. V. Nanopoulos and S. Rudaz, CERN Report No. TH-2346, 1977; R. Cahn and S. D. Ellis, Phys. Rev. D16, 1484 (1977);

- C. E. Carlson et al., Phys. Rev. Lett. 39, 908 (1977); T. Hagiwara et al., Phys. Rev. Lett. 40, 76 (1978); F. Halzen and S. Matsuda, CERN Report TH-2354 (1977); D. B. Lichtenberg et al., IUHET-23,(1977); T. Gaisser et al., Phys. Rev. D15, 2572 (1977); C. Quigg and J. Rosner, Fermilab Pub.77/82-THY (1977); M. Barnett in Proceedings of the European Conference on Particle Physics, Budapest, July, 1977.
21. R. D. Kephart et al., Phys. Rev. Lett. 39, 1440 (1977); D. M. Kaplan et al., "Study of the High Mass Dimuon Continuum in 400 GeV Proton-Nucleus Collisions", Fermilab Pub 77/107 (1977); R. L. McCarthy et al., "Atomic Number Dependence of the Production Cross Section of Massive Dihadron States", Fermilab Pub 77/102 Exp. (1977).
22. For 400 GeV protons we have used the fit from D. Kaplan et al., (Ref. 21)
- $$\left. \frac{d^2\sigma}{dm dy} \right|_{y=0} = 2.6 e^{-0.986m} s 10^{-34} \text{ dm}^2 \text{ GeV}^{-1}/\text{nucleon},$$
- which fits the data for  $5.2 < m_{\mu\mu} < 15 \text{ GeV}$ . Integrating and assuming  $\sigma_{\text{tot}} \simeq 2 \left. \frac{d\sigma}{dy} \right|_{y=0}$  we get
- $$\sigma_T(m_{\mu\mu} > 4 \text{ GeV}) = 1. \times 10^{-34} \text{ cm}^2/\text{nucleon}.$$
- See also D. Antreasyan, Phys. Rev. Lett. 39, 906 (1977), and J. Cronin, "Review of Massive Dilepton Production in Proton Nucleus Collisions", International School of Subnuclear Physics, Erice, July 1976.
23. For 225 GeV protons we have used the fit from J. B. Branson et al., (ref. 10)
- $$\text{of } \left. \frac{d\sigma}{dm} \right|_{x_F > 0.1} \simeq 1.5 m_{\mu\mu}^{-6.2} \times 10^{-30} \text{ cm}^2/\text{carbon nucleus}$$
- in the region  $1.2 < m_{\mu\mu} < 5 \text{ GeV}$ . Extrapolating the fit to higher masses and assuming that the high mass cross section goes like  $A^{1.0}$  and  $\sigma_{\text{total}} \simeq 3 \sigma(x_F > 0.1)$  we get  $\sigma_T(m_{\mu\mu} > 4 \text{ GeV}) \simeq 5.2 \times 10^{-34} \text{ cm}^2$  nucleon. For 225 GeV pions we obtain the cross section for protons by  $(d\sigma/dm) \pi^-N / (d\sigma/dm) p-N \simeq 7$  at  $m_{\mu\mu} \simeq 4 \text{ GeV}^2$
- J. G. Branson et al., Phys. Rev. Lett. 38, 1334 (1977).

24. Preliminary results from Fermilab Experiment E-444 indicate that high mass dimuon pairs are produced with a flat  $x$  distribution in pion nucleon collisions at 225 GeV.
25. S. Borenstein et al., "Measurement of the High Mass Dimuon Spectrum from 16 and 22 GeV Pions", Bulletin of Amer. Phys. Soc. 23, 65 (1978);  
A. C. Melissinas and W. Metcalf, private communication of results of BNL Experiment 687 BNL-University of Rochester collaboration.
26. M. J. Corden et al., Phys. Lett. 68B, 96 (1977).
27. Yu. M. Antipov et al., "Dimuon Production by 43 GeV/c Negative Particles", IHEP 76-42 (1976) unpublished.
28. B. Palmer, private communication.
29. J. F. Owens and E. Reya, "Hadronic Upsilon Production, Parton Distributions, and QCD" Florida State University, FSU-HEP-770920, (Oct. 1977) unpublished.
30. S. Nandi, "Scaling Laws for the Okubo-Zweig-Iizuka Violating Decays and Productions and the Interpretation of the  $\gamma$  and  $\gamma'$ " BONN-HE-77-27, (Aug. 1977) unpublished.
31. J. G. Branson et al., Phys. Rev. Lett. 38, 580 (1977); M. Binkley, et al., Phys. Rev. Lett. 37, 578 (1976).
32. See for example, Fermilab Proposal E-439 and Status Report of E-439 (May 1977), D. Garelick, Spokesperson.
33. For example, H. Lipkin (Fermilab-Conf-77/66 THY) estimates  
 $(\sigma_{pp} \rightarrow \eta_c X) \simeq 30(\sigma_{pp} \rightarrow \psi X)$  and  $BR(\eta_c \rightarrow \phi\phi) \simeq 2 BR(\psi \rightarrow \eta\phi) \simeq \frac{1}{35} BR(\psi \rightarrow \mu\mu)$ .  
Using the branching ratio  $(\phi \rightarrow 2\mu) = 2.5 \times 10^{-4}$ , we obtain  
 $\sigma_{pp} \rightarrow \eta_c \rightarrow \phi\phi \rightarrow 4\mu$  of  $10^{-39} \text{ cm}^2/\text{nucleon}$ . However, maybe the other  
 $\eta_c \rightarrow 4\mu$  and  $\eta_B \rightarrow 4\mu$  decay modes are more likely, or production cross sections with pions much larger.

34. H. T. Nieh, ITPS 87764 Stony Brook preprint "Weak Decays as Important Decay Modes of Heavy Vector Mesons With New Quantum Numbers", (1977).
35. Since the mass of the B particle is about three times the mass of the D, and since the mass of the D is about three times the mass of the K, we have scaled the distribution of the decay  $D \rightarrow K\mu\nu$  to obtain the distribution for the decay  $B \rightarrow D\mu\nu$ . This is approximately correct because the distributions depend only on the ratio of the momenta to the B and K masses. For example, Hinchliffe and Llewellyn-Smith calculate the momentum distribution for a D decay at rest to be proportional to

$$\left(\frac{P_\mu}{m_D}\right)^2 \left[1 - \left(\frac{m_K}{m_D}\right)^2 - 2 \left(\frac{P_\mu}{m_D}\right)^2\right] \left(1 - 2 \frac{P_\mu}{m_D}\right).$$

36. D. Sivers, Nucl. Phys. B106, 95 (1976).
37. M. Bourguin and J. M. Gaillard, Nucl. Phys. B114, 334 (1976).
38. We assume a 12%  $D \rightarrow k\mu\nu$  branching ratio.
- a.  $2\mu$  background,  $\sigma_{2\mu} = 4\mu\text{b/nucleon}$ . We have 3.5% to 10% unidentified  $2\mu$  events. We determine this background to 10% of its value. We add missing energy requirement of 20 GeV. We get a reduction of the signal by a factor of 2 and a reduction of the background by a factor of 10. We also get a factor of 2 rejection by not including the very low  $P_t$  region

$$\sigma_{\text{charm}} \geq \frac{4\mu\text{b} \times 0.01 \times 0.10 \times 0.5}{0.5 \times 0.12} = 0.3 \times 10^{-32} \text{ cm}^2/\text{nucleon}$$

- b. Decay backgrounds. The level of  $\pi$  decay muons for  $E_\mu \geq 20$  GeV is about the same as that from  $2\mu$  events. The density comparison allows us to determine the  $\pi$  decay to 10% of its value. A missing energy of 20 GeV requirement will yield another factor of 5 rejection (since for  $\pi$  decay  $\langle E_\nu \rangle \simeq \frac{1}{4} \langle E_\mu \rangle$  while for charm 3 body decay  $\langle E_\nu \rangle \simeq \langle E_\mu \rangle$ ). An additional factor of 2 rejection is obtained by not including the very low  $P_t$  region

$$\sigma_{\text{charm}} \geq \frac{4\mu\text{b} \times 0.1 \times 0.2 \times 0.5}{0.12} = 3 \times 10^{-31} \text{ cm}^2/\text{nucleon}.$$

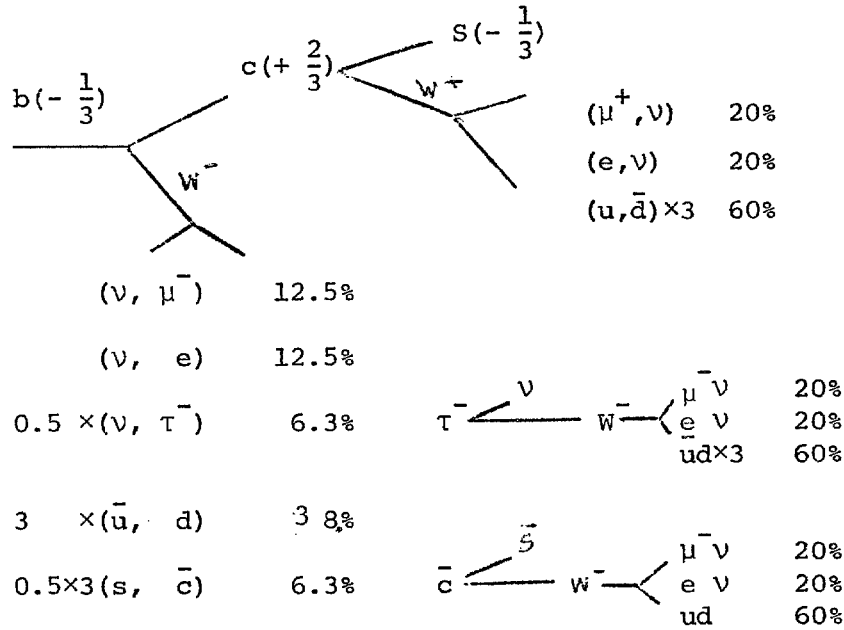
39. By requiring 40 GeV in missing energy we reduce the background from normal  $2\mu$  events by  $3 \times 10^{-3}$  and reduce the signal by a factor of 2. We expect to know the background to 10% of its value and to obtain an additional factor of 3 rejection by eliminating low mass pairs

$$\sigma_{\text{charm}} \geq \frac{4\mu\text{b} \times 3 \times 10^{-3} \times 0.1}{3 \times 0.5 \times (0.12)^2} = 0.6 \times 10^{-31} \text{cm}^2/\text{nucleon}$$

40. The topologies and fractions for tau lepton production are expected to be the same as those for charm except for the missing energy which is larger due to the presence of additional neutrinos in the final state. However, the low  $P_t$  singly produced muons are expected to be predominantly from charm. This is because the cross sections for tau lepton production are a factor of  $10^4$  smaller than the charm production cross sections. We estimated the tau lepton cross sections under the assumption that they are equal to the total dimuon cross section above  $m_{\mu\mu} = 2 m_\tau = 4$  GeV. Using the available dimuon data we estimate cross sections of roughly  $1 \times 10^{-34} \text{cm}^2/\text{nucleon}$  for 400 GeV protons<sup>22</sup>, about  $0.5 \times 10^{-34} \text{cm}^2/\text{nucleon}$  for 225 GeV protons<sup>23</sup>, and about  $4 \times 10^{-34} \text{cm}^2/\text{nucleon}$  for 225 GeV negative pions. This last cross section is four orders of magnitude smaller than our calculated value of  $3.2 \times 10^{-30} \text{cm}^2/\text{nucleon}$  for charm production by 225 GeV negative pions. We can, therefore, neglect the tau contribution to the low  $P_t$  singly produced muon signal.
41. Results of Delco collaboration BR ( $D \rightarrow \mu\nu$ ) of  $12\% \pm 2\%$ , S. Wojcicki private communication.

Appendix A - Decay modes of Bottom quarks

We assume that a Cabibbo like angle couples the bottom quark predominantly to a charmed quark. We use quark counting to estimate branching ratios. The hadronic decay modes are enhanced by a factor of 3 due to color. We also assume a 0.5 factor suppression due to phase space for those decays involving the heavy charmed quark or the heavy  $\tau$  lepton in the final state



The direct leptons from the b quark decay are expected to have high  $P_t$ . The leptons from the charm and  $\tau$  lepton decay are expected to have medium  $P_t$ . By taking various combinations we obtain that 29% of the decays involve at least one muon in the final state, another 29% involving electrons, neutrinos and hadrons but no muon and a final 42% hadronic decay.

These are summarized below.

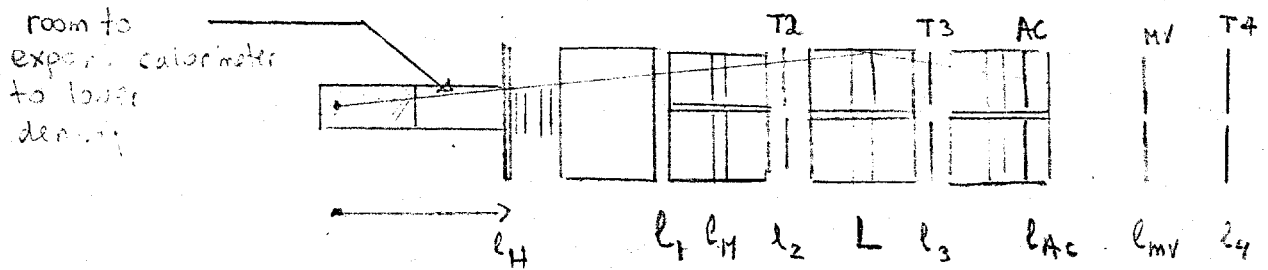
Single decay  $b(-\frac{1}{3})$

$\mu^-$ high $P_t$ + neutrinos, X	10%	
$\mu^-$ medium $P_t$ " " , X	3.1%	
$\mu^+$ medium $P_t$ + " " , X	12%	
$\mu^+ \mu^-$ + neutrinos , X	3.5%	
hadrons, e, neutrinos	29%	} 71%
hadrons	42%	

Combining the decays of the bottom and bottom mesons we obtain

single $\mu^-$	- 18.1% (7.1% high $P_t$ , 11% medium $P_t$ )
single $\mu^+$	- 18.1% (7.1% high $P_t$ , 11% medium $P_t$ )
$\mu^+ \mu^-$	- 8.4%
$\mu^- \mu^-$	- 1.6%
$\mu^+ \mu^+$	- 1.6%
3 $\mu$	- 2%
4 $\mu$	- 0.1%
no muons	- 50%

Appendix B : Acceptance Calculations



Hodoscope size is 12'x12' all other counters T2, T3, T4, AC and MV are 10'x10'.

A space is left behind the fine grain calorimeter such that the calorimeter's density can be expanded while retaining the interaction point fixed in space for identical acceptance at all densities. The following are the distances in feet from the interaction point of the various acceptance defining counters.

- $l_H = 15'$  Hodoscope, large angle muon identifier
- $l_1 = 28'$  Beginning of first toroid
- $l_M = 32'$  Middle of first toroid (momentum determination)
- $L = 44'$  middle of spectrometer system
- $l_{AC} = 59'$  High Pt acrylic trigger, end of third toroid
- $l_{MV} = 67'$  High Pt movable trigger counter
- $l_{T4} = 87'$  Last high Pt trigger counter

The energy loss in all the steel (8 meters) is  $\Delta = 12$  GeV. The transverse position  $x_i$  in counter  $i$  at  $z$  position  $l_i$  is determined (including  $de/dx$  energy loss) by the following approximate equation:

$$\frac{P_t}{P_{||}} l_i \pm \frac{M (l_i - L)}{P_{||} - \Delta} \approx x_i \quad (B1)$$

where  $M$  is the  $P_t$  kick of the magnet (2.2 GeV), and the  $\pm$  depends on the muon's charge. The  $P_t$  cut determined by counter  $i$  for focussing particles is obtained by setting  $x_i$  to zero in the above equation ( i.e. the ray crossing the median plane)

$$P_t \geq \frac{M (l_i - L)}{l_i (1 - \Delta/P_{||})} = P_{t \text{ cut}}^{\infty} \left( \frac{1}{1 - \Delta/P_{||}} \right) \quad (B2)$$

The  $de/dx$  energy loss is important at low energy and transforms a sharp  $P_t$  cut into a fuzzy one. We list the  $P_t$  cuts for the last three counters in the apparatus.

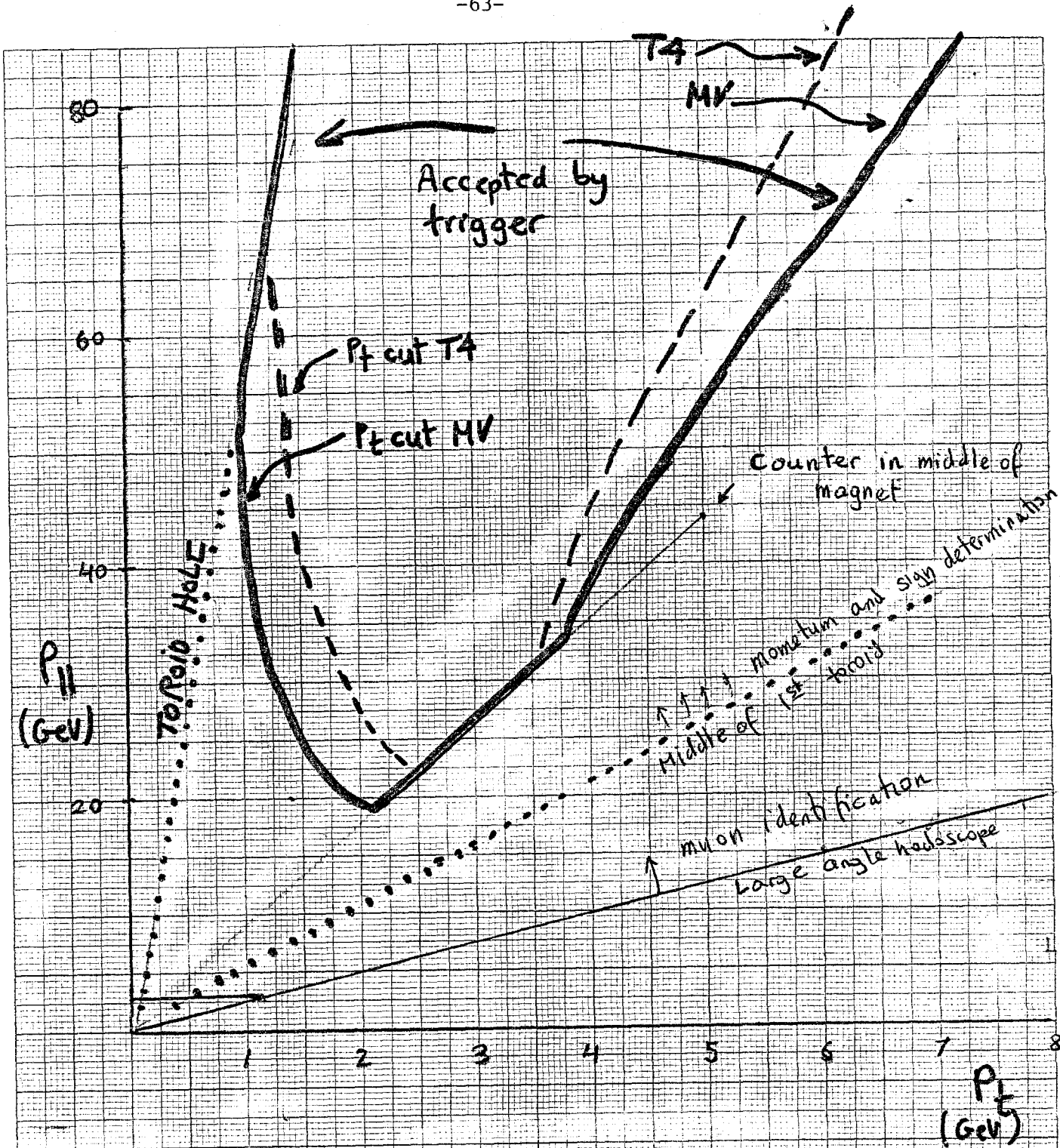
Counter	$P_t^{\infty}$ cut	$P_t^{50 \text{ GeV}}$ cut	$P_t^{20 \text{ GeV}}$ cut
AC	0.56 GeV	0.74 GeV	1.4 GeV
MV	0.76 GeV	1.00 GeV	1.9 GeV
T4	1.10 GeV	1.45 GeV	2.8 GeV

Lower  $P_t$  cuts may be obtained by requiring muons only not to cross at T3 or T2.

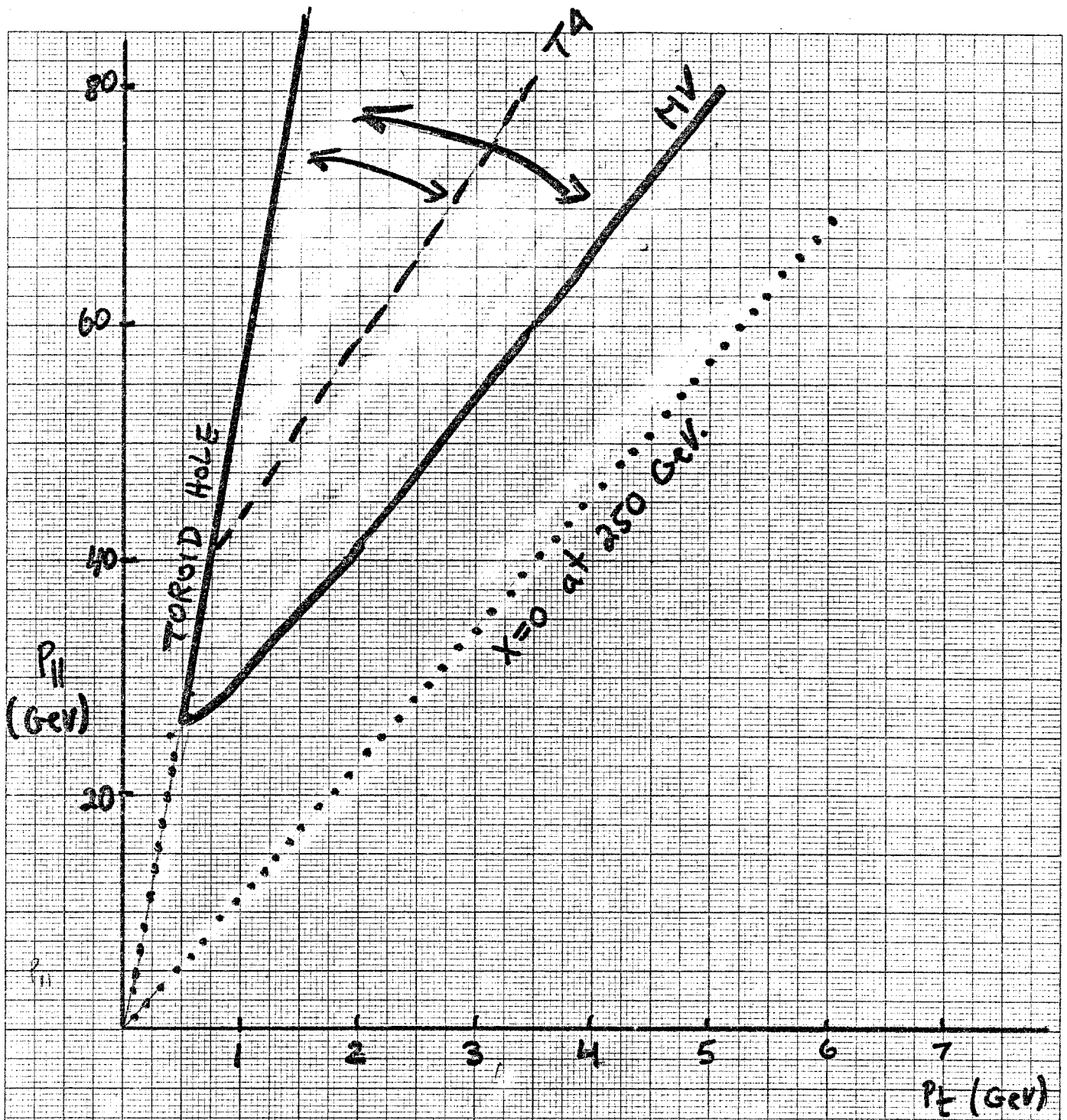
Figure 11 shows the boundary of the various counters on a  $P_t$  vs  $P$  plot in the lab frame for focussing muons. A similar plot for defocussing muons is shown in figure 12. The counter boundaries for the case of focussing muons is shown in the center of mass of 250 GeV pion-nucleon system. As can be seen in the figure ( figure 13) the acceptance of the  $P_t$  trigger covers almost the entire forward hemisphere and a large fraction of the backwards hemisphere.

The acceptance for detection of second muons is also very large. Only 6% of  $4\pi$  is missed. For the events that are missed just outside the boundary of the hodoscope we have  $P_{lab} \leq 2.7 P_t$ . So the majority of those muons have such low an energy that they would range out anyway before they reach the hodoscope.

As for measuring the sign and momentum of second muons, the muons must reach the middle of the first toroid. Only 18% of  $4\pi$  in the backwards hemisphere fail to do so, and an additional 3.6% of  $4\pi$  in the forward hemisphere do not go through the hole and therefore have a poor momentum determination or none at all (if they traverse the hole all the way to the third toroid).



Acceptance of various counters  
lab system: focussing muons.



Acceptance of various counters  
lab system: defocussing muons.  
Additional counters may be used  
to further discriminate against low  $p_{\perp}$   
defocussing muons.

